B-mode foregrounds removal

Mathieu Remazeilles

The University of Manchester

CMB Foregrounds Workshop – UCSD
San Diego, USA, 29 Nov – 1 Dec 2017

Outline

- Primordial CMB B-mode
- Sunyaev-Zeldovich effect
- Optimization (another time)?

CMB B-mode vs foregrounds

Remazeilles, Banday, Baccigalupi, et al,
for the CORE collaboration – JCAP 2017 accepted

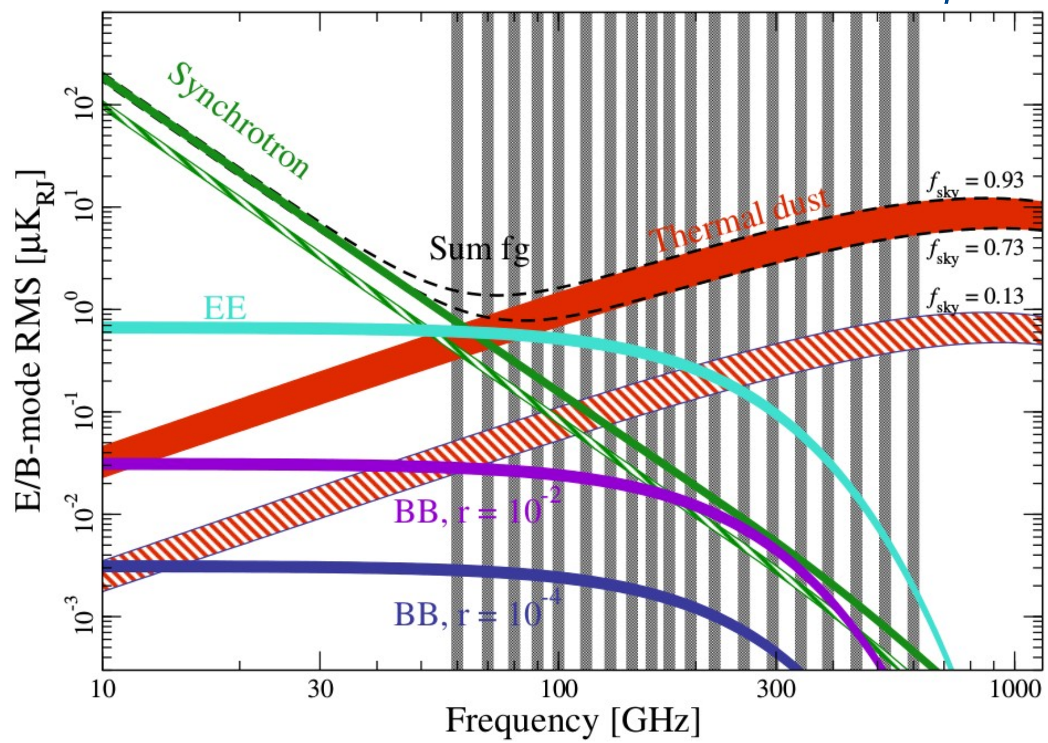

- Polarization **less complex** than intensity (fewer components) but **more challenging:**
  - → larger dynamic range between CMB and foregrounds!
  - → a slight mis-modelling of foregrounds can have a dramatic impact on the CMB B-mode
- **Foregrounds cannot be avoided just by limiting the frequency range of observations:**
  - → At 300 GHz the synchrotron has same amplitude and color than the CMB B-mode $r=10^{-2}$!
  - → **Broad frequency range is essential** to fight against spectral degeneracies

Component separation algorithms

- COMMANDER – *Eriksen et al 2004, 2008 ; Remazeilles et al 2016, 2017*

  Bayesian parametric fitting in pixel space through MCMC Gibbs sampling

- SMICA – *Delabrouille et al 2003 ; Cardoso et al 2008*

  Blind power spectrum fitting in harmonic space

- NILC – *Delabrouille et al 2009 ; Remazeilles et al 2011 ; Basak et al 2012, 2013*

  Minimum-variance internal linear combination in wavelet space

- X-FORECAST – *Errard et al 2016 ; Stompor et al 2016*

  Parametric fitting of foreground mixing matrix plus linear combination

---

The first three techniques have been successfully employed on Planck data!
– Planck 2015 results. IX., A&A 2016

Those four techniques have been tested on CORE simulations for CMB B-mode forecasts
– Remazeilles et al, for the CORE collaboration, JCAP 2017

CORE

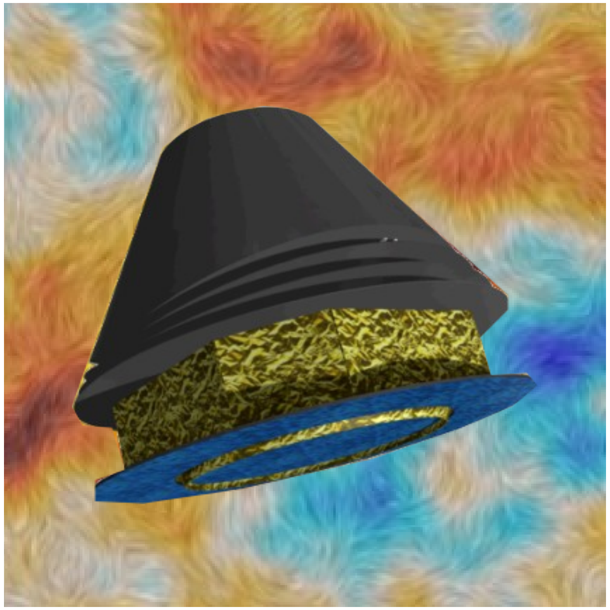

→ *Not selected by ESA, but we have cleared the path on the B-mode challenges!*

→ *Ten papers (JCAP special issue)*

- Mission: Delabrouille, de Bernardis, Bouchet et al.
- Instrument: de Bernardis, Ade, Baselmans et al.

- Inflation: Finelli, Bucher, Achucarro et al.
- Lensing: Challinor, Allison, Carron, et al.
- Parameters: Di Valentino, Brinckmann, Gerbino et al.
- Clusters: Melin, Bonaldi, Remazeilles et al.
- Velocity: Burigana, Carvalho, Trombetti et al.
- Sources: De Zotti, Gonzalez-Nuevo, Lopez-Caniego et al.

- Foregrounds: Remazeilles, Banday, Baccigalupi et al.
- Systematics: Natoli, Ashdown, Banerji et al.

Exploring Cosmic Origins with CORE: B-mode Component Separation

M. Remazeilles,[1] A. J. Banday,[2,3] C. Baccigalupi,[4,5] S. Basak,[6,4] A. Bonaldi,[1] G. De Zotti,[7] J. Delabrouille,[8] C. Dickinson,[1] H. K. Eriksen,[9] J. Errard,[10] R. Fernandez-Cobos,[11] U. Fuskeland,[9] C. Hervías-Caimapo,[1] M. López-Caniego,[12] E. Martinez-González,[11] M. Roman,[13] P. Vielva,[11] I. Wehus,[9] A. Achucarro,[14,15] P. Ade,[16] R. Allison,[17] M. Ashdown,[18,19] M. Ballardini,[20,21,22] R. Banerji,[8] N. Bartolo,[23,24,7] J. Bartlett,[8] D. Baumann,[25] M. Bersanelli,[26,27] M. Bonato,[28,4] J. Borrill,[29] F. Bouchet,[30] F. Boulanger,[31] T. Brinckmann,[32] M. Bucher,[8] C. Burigana,[21,33,22] A. Buzzelli,[34,35,36] Z.-Y. Cai,[37] M. Calvo,[38] C.-S. Carvalho,[39] G. Castellano,[40] A. Challinor,[25] J. Chluba,[1] S. Clesse,[32] I. Colantoni,[40] A. Coppolecchia,[34,41] M. Crook,[42] G. D'Alessandro,[34,41] P. de Bernardis,[34,41] G. de Gasperis,[34,36] J.-M. Diego,[11] E. Di Valentino,[30,43] S. Feeney,[18,44] S. Ferraro,[45] F. Finelli,[21,22] F. Forastieri,[46] S. Galli,[30] R. Genova-Santos,[47,48] M. Gerbino,[49,50] J. González-Nuevo,[51] S. Grandis,[52,53] J. Greenslade,[18] S. Hagstotz,[52,53] S. Hanany,[54] W. Handley,[18,19] C. Hernandez-Monteagudo,[55] M. Hills,[42] E. Hivon,[30] K. Kiiveri,[56,57] T. Kisner,[29] T. Kitching,[58] M. Kunz,[59] H. Kurki-Suonio,[56,57] L. Lamagna,[34,41] A. Lasenby,[18,19] M. Lattanzi,[46] J. Lesgourgues,[32] A. Lewis,[60] M. Liguori,[23,24,7] V. Lindholm,[56,57] G. Luzzi,[34] B. Maffei,[31] C.J.A.P. Martins,[61] S. Masi,[34,41] D. McCarthy,[62] J.-B. Melin,[63] A. Melchiorri,[34,41] D. Molinari,[33,46,21] A. Monfardini,[38] P. Natoli,[33,46] M. Negrello,[16] A. Notari,[64] A. Paiella,[34,41] D. Paoletti,[21] G. Patanchon,[8] M. Piat,[8] G. Pisano,[16] L. Polastri,[33,45] G. Polenta,[65,66] A. Pollo,[67] V. Poulin,[32,68] M. Quartin,[69,70] J.-A. Rubino-Martin,[47,48] L. Salvati,[34,41] A. Tartari,[8] M. Tomasi,[26] D. Tramonte,[47] N. Trappe,[62] T. Trombetti,[21,33,22] C. Tucker,[16] J. Valiviita,[56,57] R. Van de Weijgaert,[71,72] B. van Tent,[73] V. Vennin,[74] N. Vittorio,[35,36] K. Young,[54] and M. Zannoni,[75,76] for the CORE collaboration.

Accepted by JCAP (2017)

Reconstruction of the primordial B-mode with CORE

r = 5 x 10^{-3}, without lensing

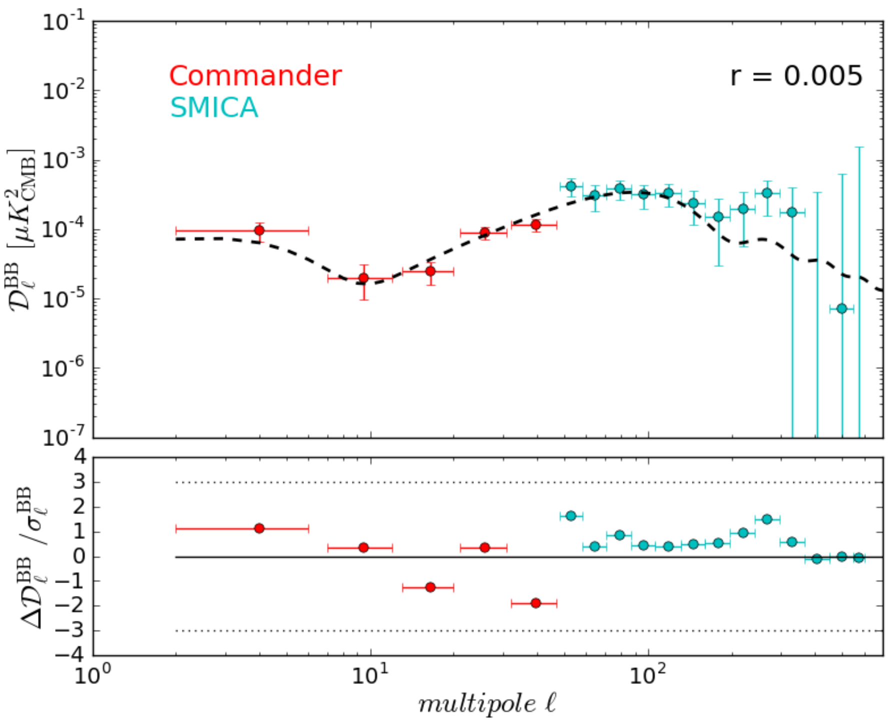

10σ detection after foreground cleaning

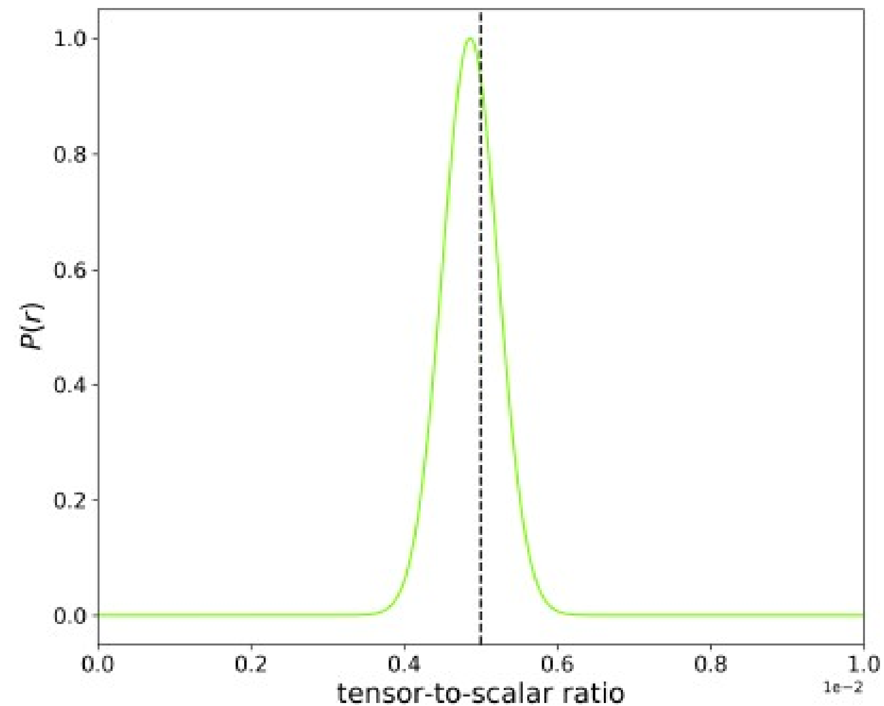

Remazeilles, Banday, Baccigalupi, et al, for the CORE collaboration, 2017

<u>Foregrounds</u>: thermal dust MBB, synchrotron power-law, AME 1% polarized,
with variable spectral indices/temperatures over the sky

Reconstruction of the primordial B-mode with CORE

r = 5 x 10^{-3}, with lensing

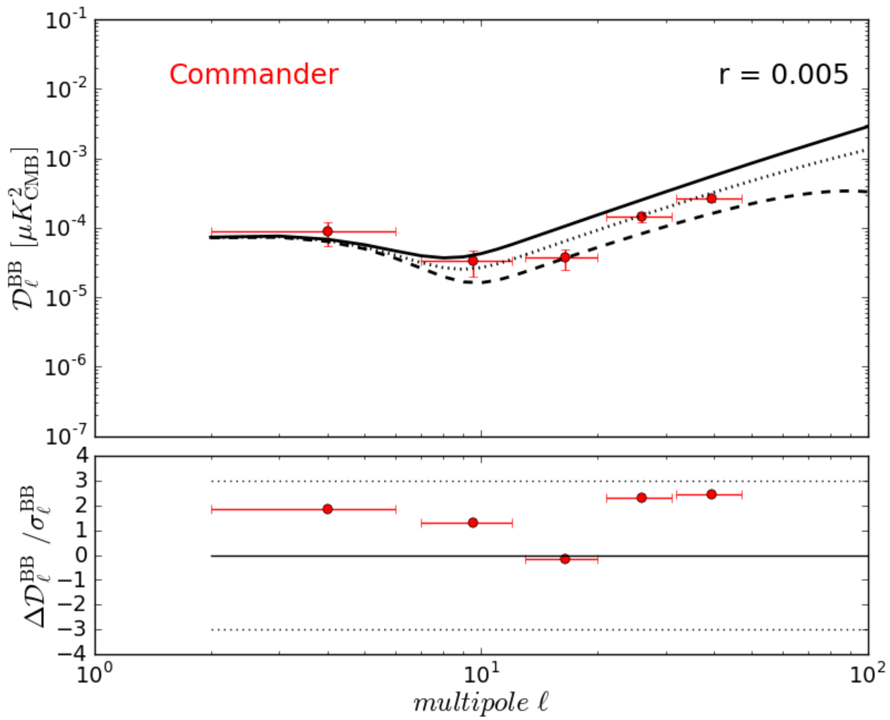

4σ detection after foreground cleaning and 60% delensing

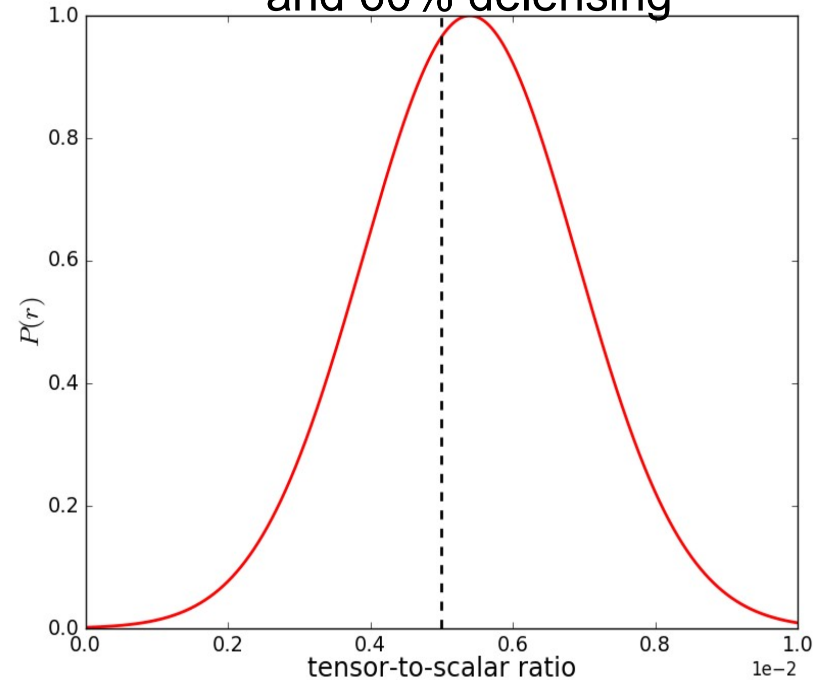

Remazeilles, Banday, Baccigalupi, et al, for the CORE collaboration, 2017

<u>Foregrounds</u>: thermal dust MBB, synchrotron power-law, AME 1% polarized, with variable spectral indices/temperatures over the sky

Reconstruction of the primordial B-mode with CORE

r = 1 x 10^{-3}, without lensing

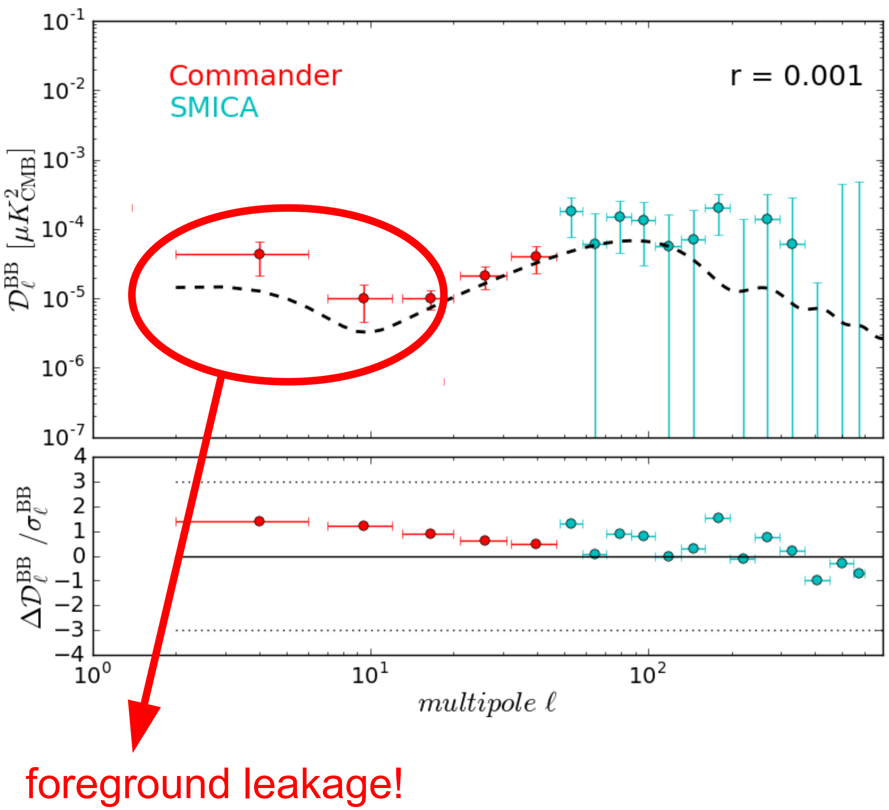

3σ bias after foreground cleaning

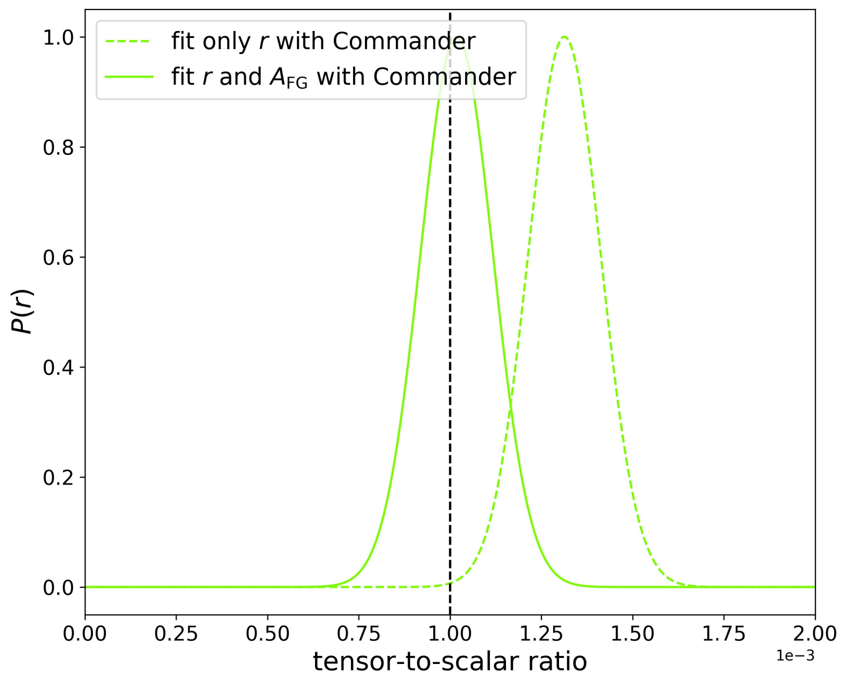

Remazeilles, Banday, Baccigalupi, et al, for the CORE collaboration, 2017

<u>Foregrounds</u>: thermal dust MBB, synchrotron power-law, AME 1% polarized, with variable spectral indices/temperatures over the sky

Probe mission study: PICO

- 21 frequency bands between 21 – 800 GHz
- Overall sensitivity of ~ 1 μK.arcmin

CMBP						
del nu/nu	0,25		del center	1,2		
nu1	30	GHz				
	nu	**nu_low**	**nu_high**	**del nu**	**FWHM**	**PolWeight**
Band#	**(GHz)**	**(GHz)**	**(GHz)**	**(GHz)**	**(arcmin)**	**(uk*arcmin)**
1	21	18,2	23,4	5,2	40,9	50
2	25	21,9	28,1	6,3	34,1	33
3	30	26,3	33,8	7,5	28,4	22,4
4	36,0	31,5	40,5	9,0	23,7	15
5	43,2	37,8	48,6	10,8	19,7	9,1
6	51,8	45,4	58,3	13,0	16,4	7
7	62,2	54,4	70,0	15,6	13,7	5
8	74,6	65,3	84,0	18,7	11,4	4
9	89,6	78,4	100,8	22,4	9,5	3,2
10	107,5	94,1	120,9	26,9	7,9	2,9
11	129,0	112,9	145,1	32,2	6,6	2,7
12	154,8	135,4	174,1	38,7	5,5	2,6
13	185,8	162,5	209,0	46,4	4,6	3,6
14	222,9	195,0	250,8	55,7	3,8	5,3
15	267,5	234,0	300,9	66,9	3,2	9
16	321,0	280,9	361,1	80,2	2,7	16,0
17	385,2	337,0	433,3	96,3	2,2	32
18	462,2	404,4	520,0	115,6	1,8	75
19	554,7	485,3	624,0	138,7	1,5	220,0
20	665,6	582,4	748,8	166,4	1,3	1100
21	798,7	698,9	898,5	199,7	1,1	10000,0

PICO PSM simulation: Stokes Q maps

Thermal dust, 353 GHz

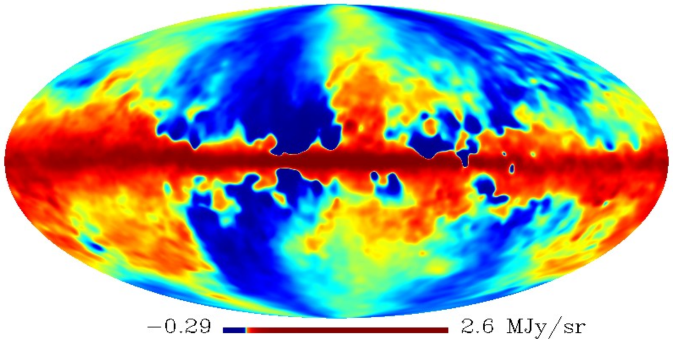

Dust spectral index

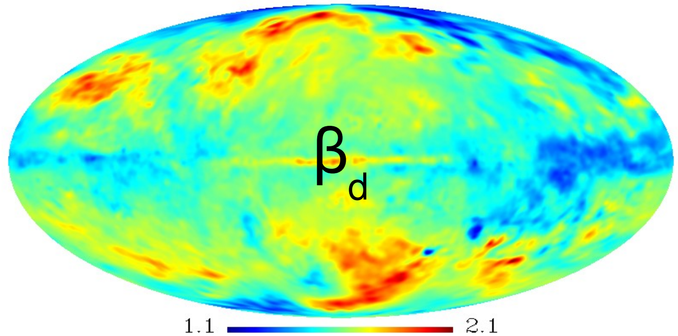

Dust temperature

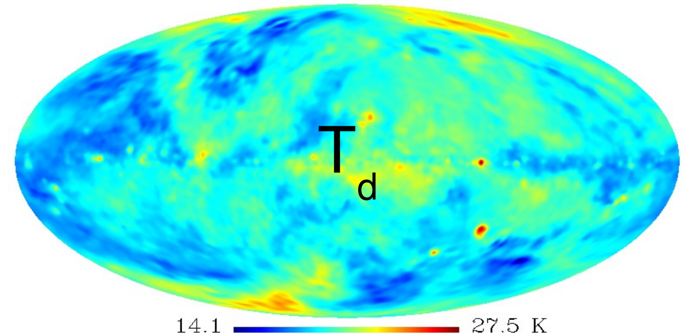

Synchrotron, 23 GHz

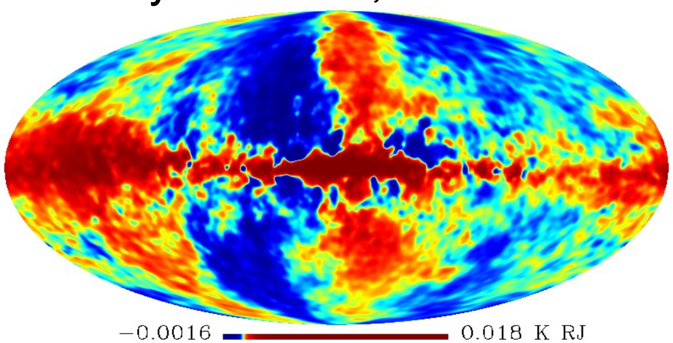

Synchrotron spectral index

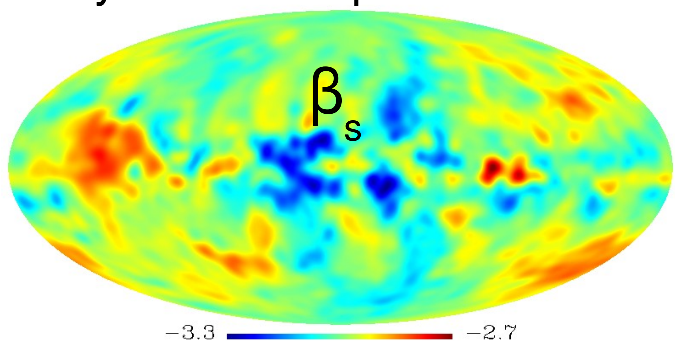

Synchrotron curvature

uniform $C_s = 0.3$

Lensed CMB

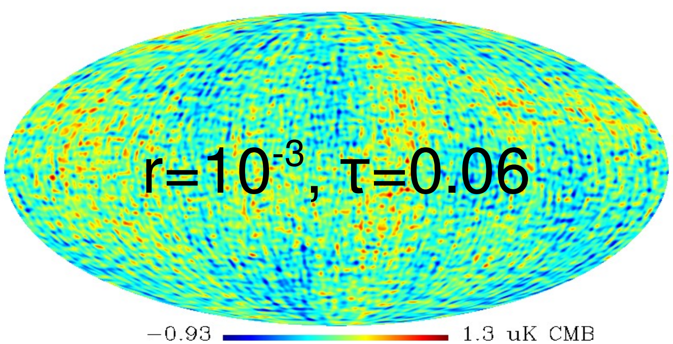

smoothed to 1°
for illustration purposes

Based on the Planck Sky Model (PSM) – *Delabrouille et al 2013*

Methodology

Eriksen et al 2004, 2008
Remazeilles et al 2016, 2017

1. Separation of components (`COMMANDER` fitting + Gibbs sampling):

$$\boldsymbol{s}^{(i+1)} \leftarrow P\left(\boldsymbol{s} \middle| C_\ell^{(i)}, \boldsymbol{\beta}^{(i)}, \boldsymbol{d}\right),$$

Amplitudes (CMB, foregrounds)

$$C_\ell^{(i+1)} \leftarrow P\left(C_\ell \middle| \boldsymbol{s}^{(i+1)}\right),$$

Power spectra (CMB)

$$\boldsymbol{\beta}^{(i+1)} \leftarrow P\left(\boldsymbol{\beta} \middle| \boldsymbol{s}^{(i+1)}, \boldsymbol{d}\right),$$

Spectral indices (foregrounds)

2. Likelihood estimation of r and A_{lens}:

$$-2\ln\mathcal{L}\left[\widehat{C}_\ell | C_\ell^{th}\left(r, A_{lens}\right)\right] = \sum_\ell (2\ell+1)\left[\ln\left(\frac{C_\ell^{th}}{\widehat{C}_\ell}\right) + \frac{C_\ell^{th}}{\widehat{C}_\ell} - 1\right]$$

$$C_\ell^{th} = r\, C_\ell^{tensor}(r=1) + A_{lens}\, C_\ell^{lensing}(r=0).$$

3. Blackwell-Rao posterior: $\mathcal{P}\left(r, A_{lens}\right) \approx \frac{1}{N}\sum_{i=1}^{N}\mathcal{L}\left[\widehat{C}_\ell^i | C_\ell^{th}\left(r, A_{lens}\right)\right]$

Results for 3D foregrounds ($r = 10^{-3}$ + lensing)

β_d, T_d, β_s, Cl^{EE}, Cl^{BB} locally fitted **(No synchrotron curvature)**

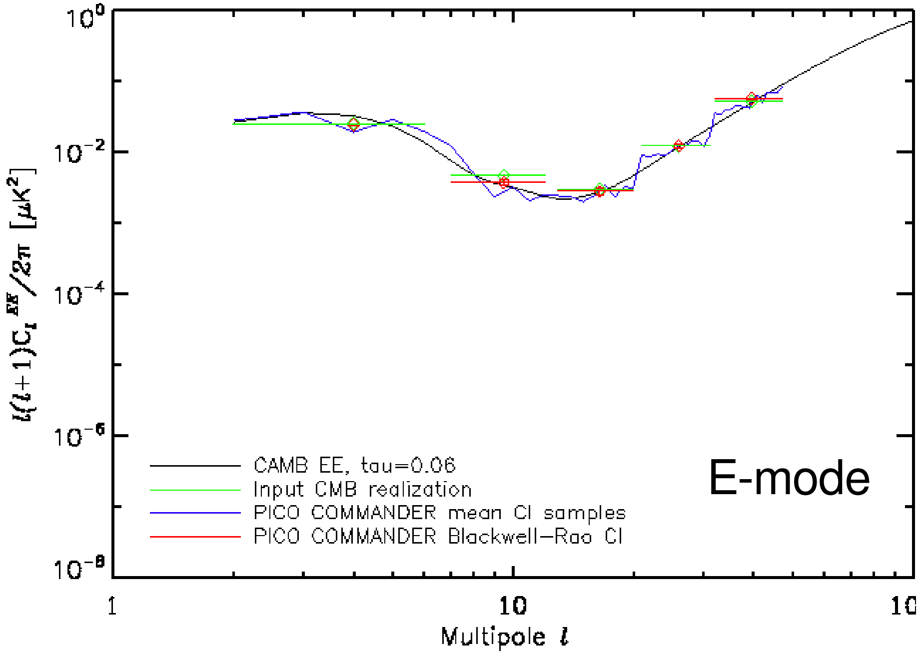

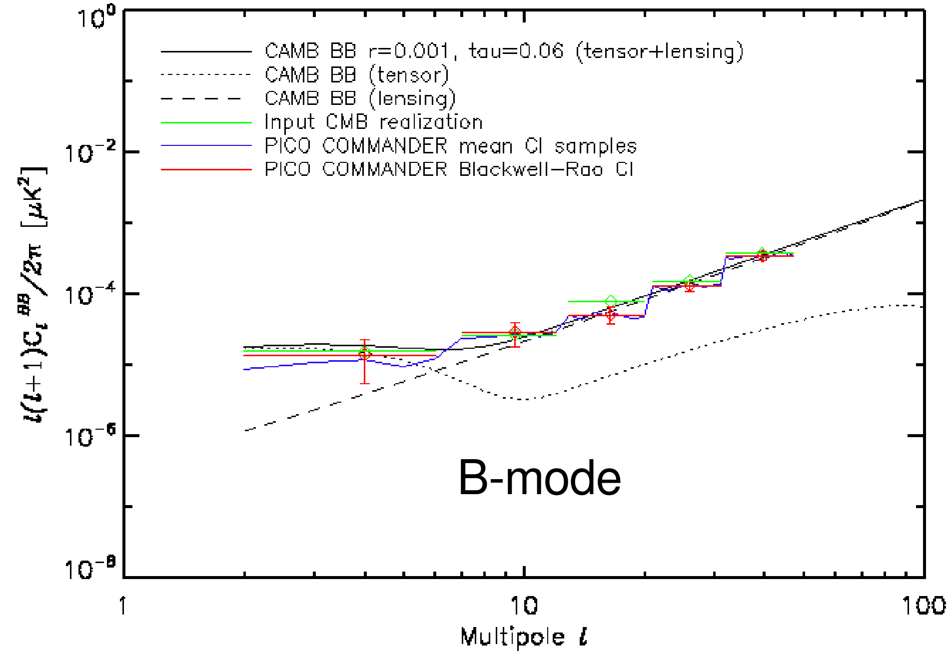

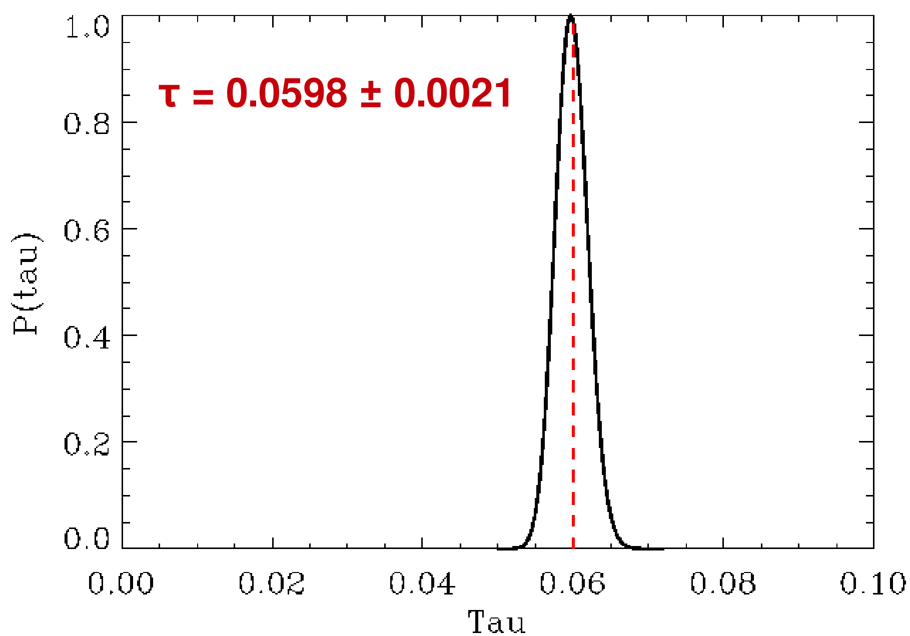

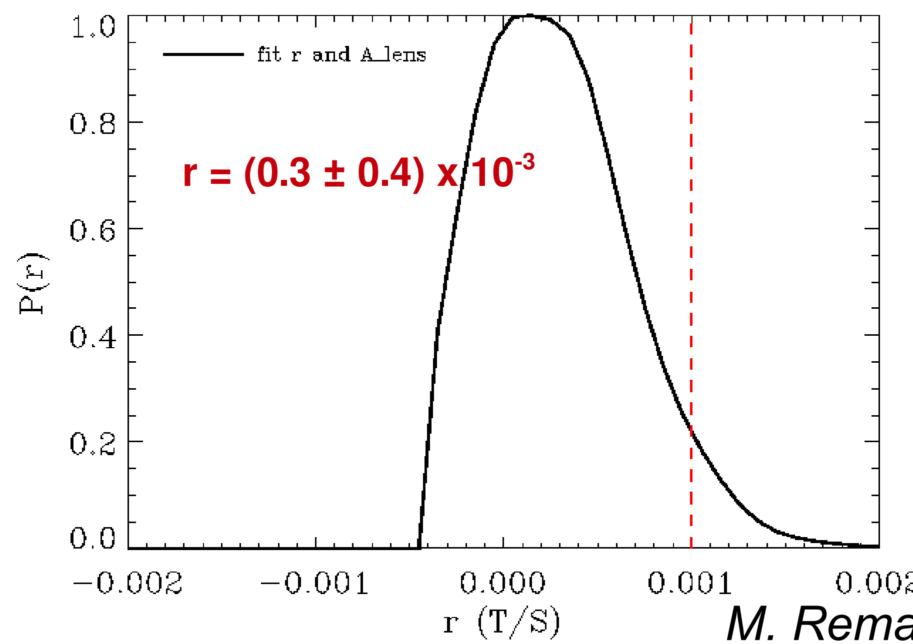

M. Remazeilles

Results for 4D foregrounds (r = 10^{-3} + lensing)

β_d, T_d, β_s, Cl ^{EE}, Cl ^{BB} locally fitted, C_s globally fitted

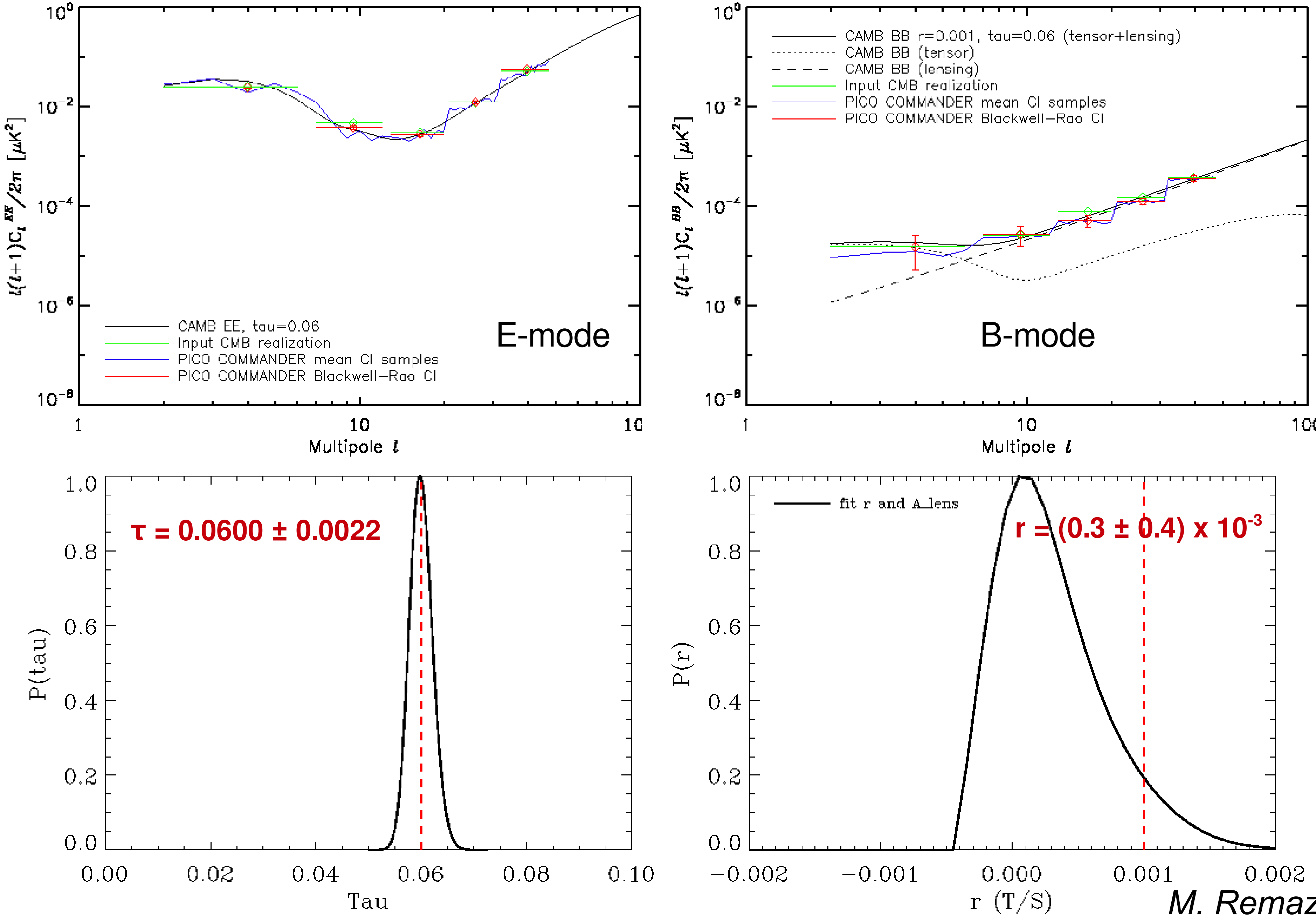

M. Remazeilles

PICO without 21, 25, 665, 800 GHz

β_d, T_d, β_s, Cl^{EE}, Cl^{BB} locally fitted, C_s globally fitted

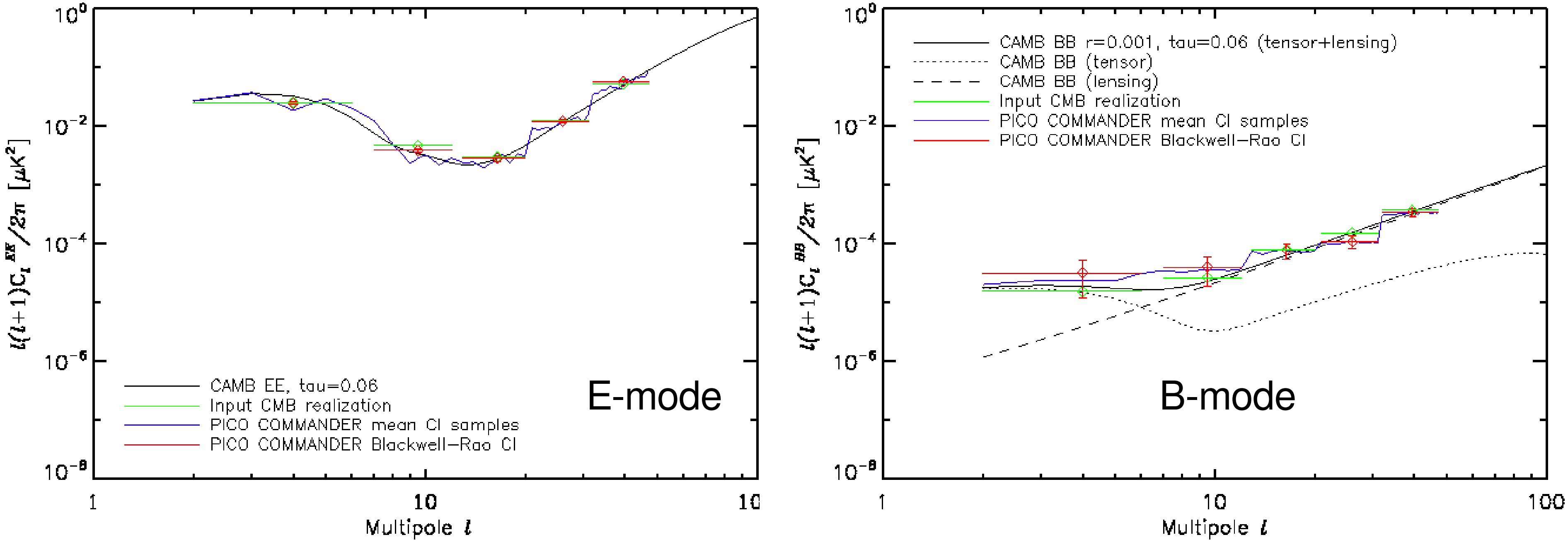

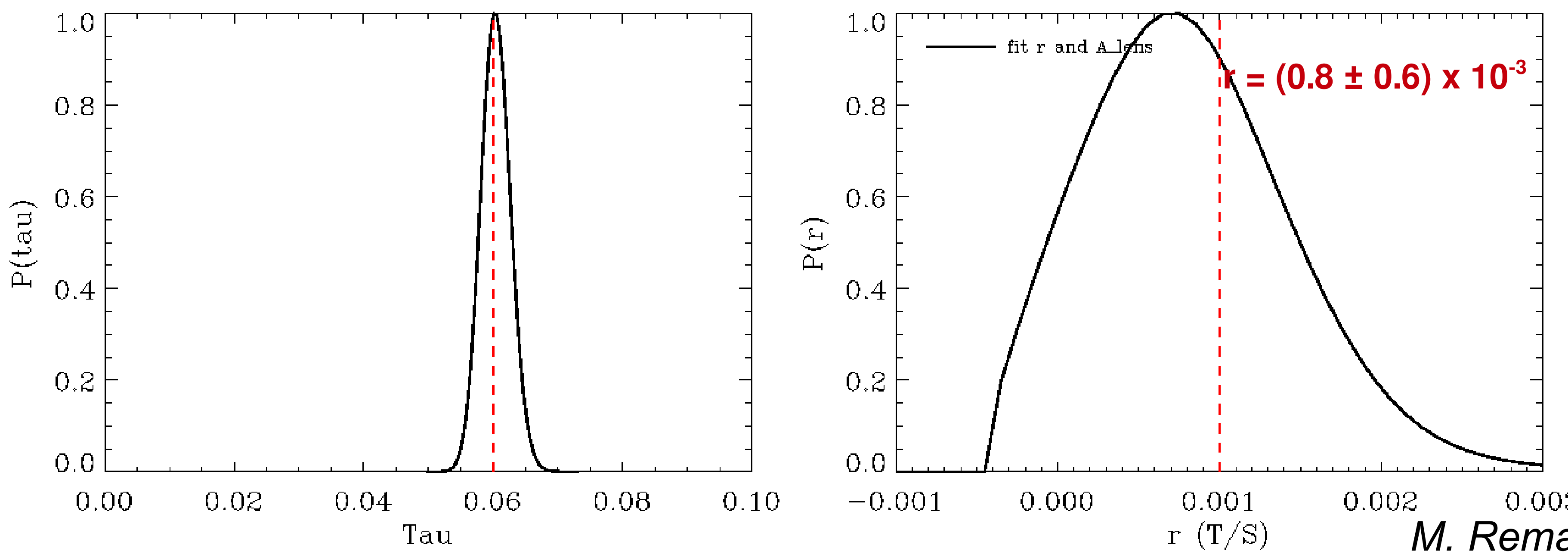

M. Remazeilles

PICO 43 – 462 GHz

β_d, T_d, β_s, Cl^{EE}, Cl^{BB} locally fitted, C_s globally fitted

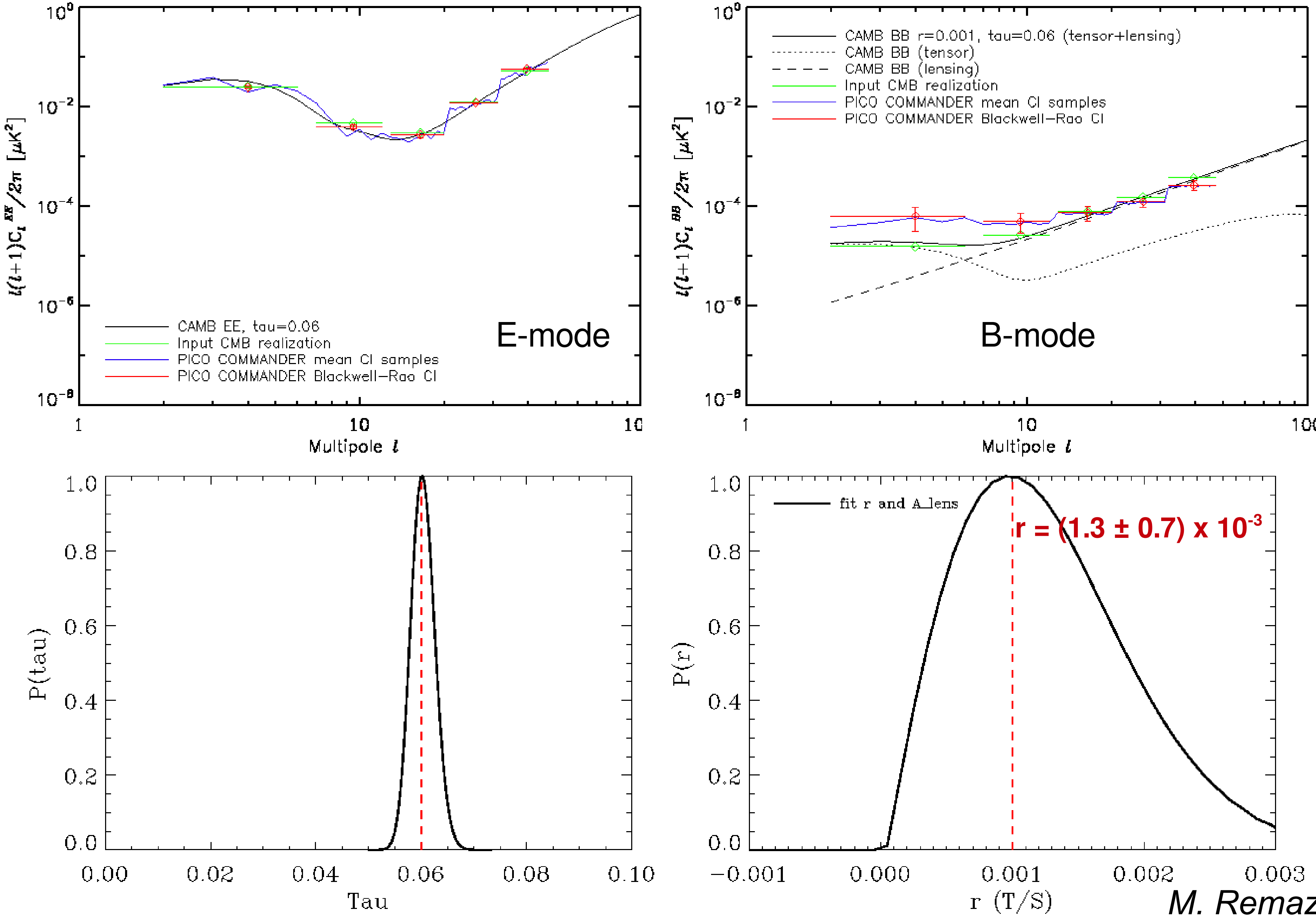

M. Remazeilles

Results for 4D foregrounds
Full PICO

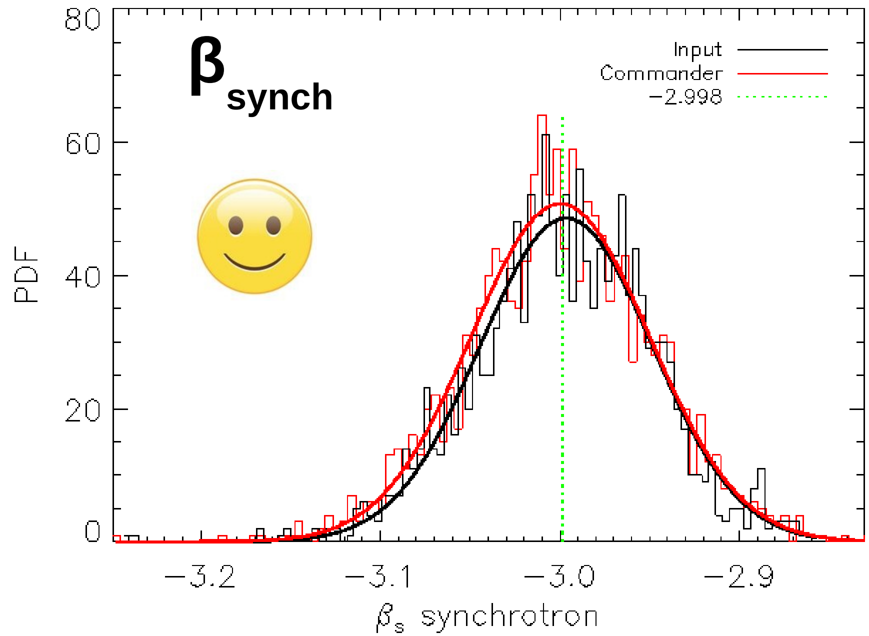

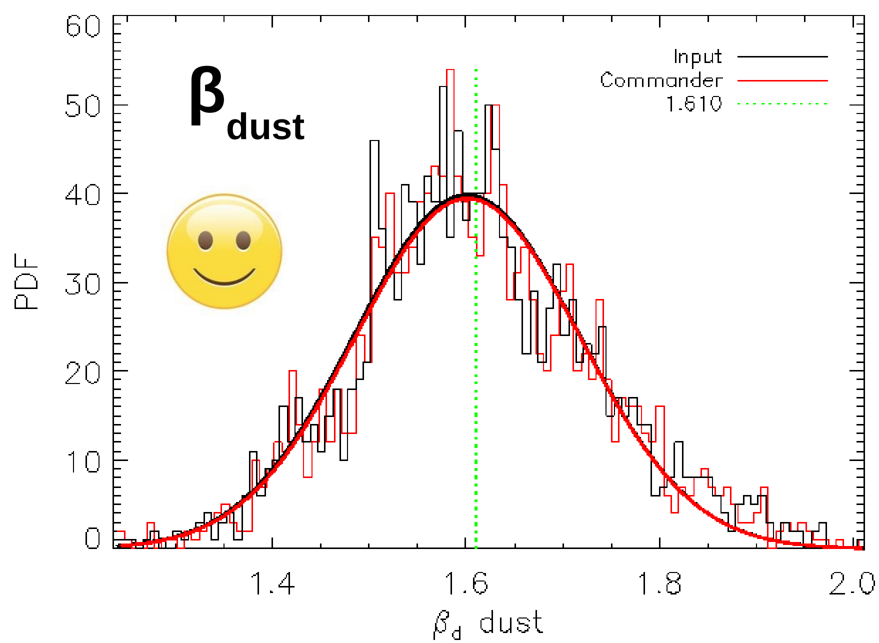

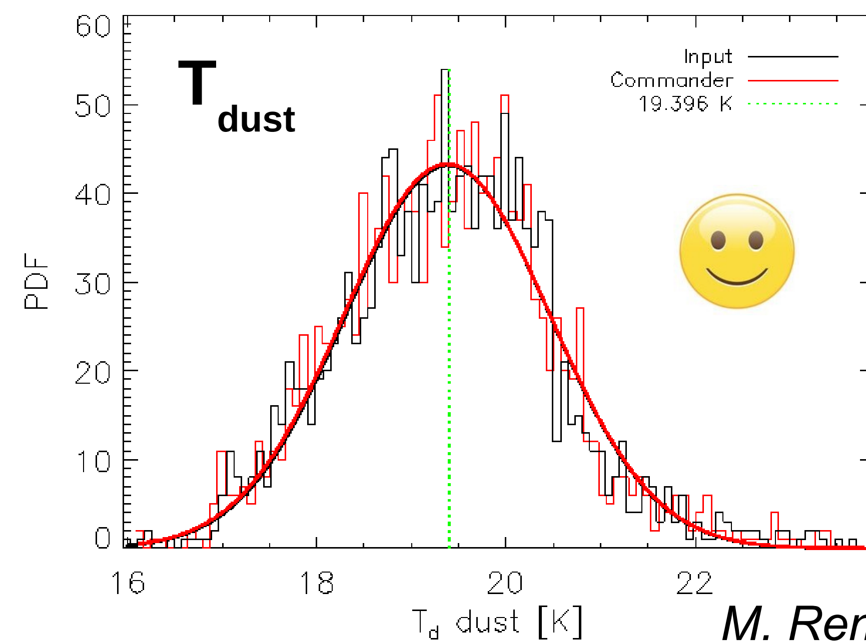

M. Remazeilles

Results for 4D foregrounds
PICO without 21, 25, 665, 800 GHz

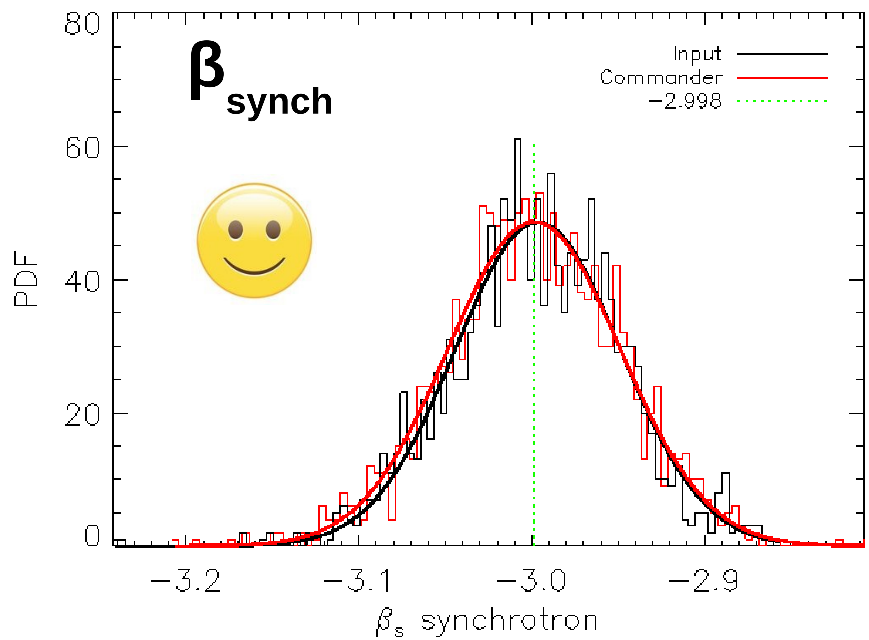

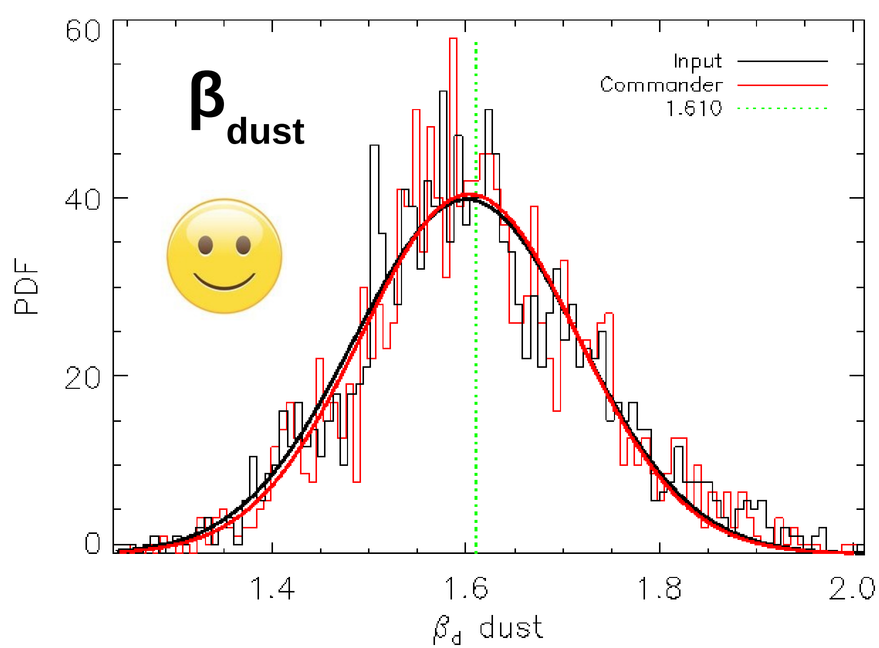

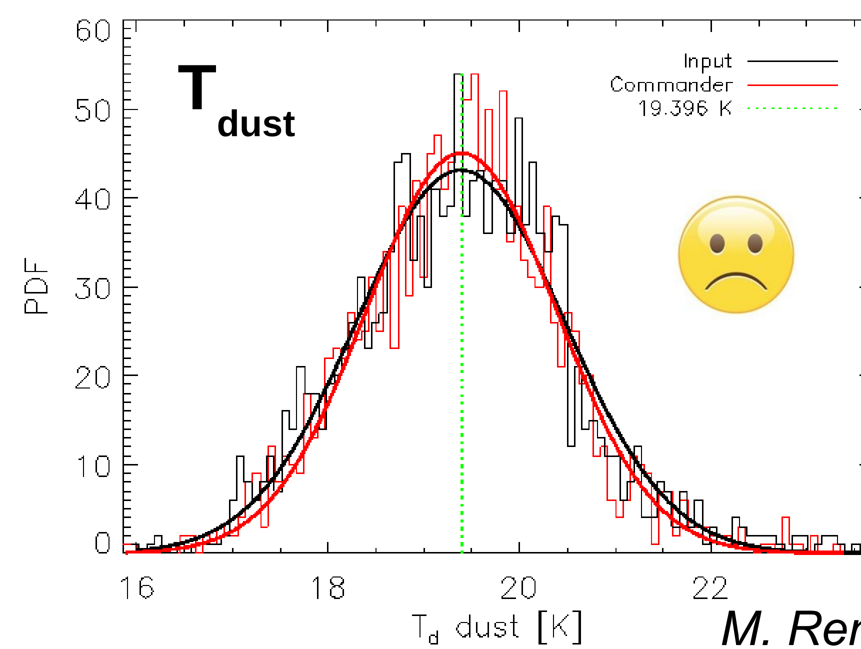

M. Remazeilles

Results for 4D foregrounds (C_s global)
43 – 462 GHz

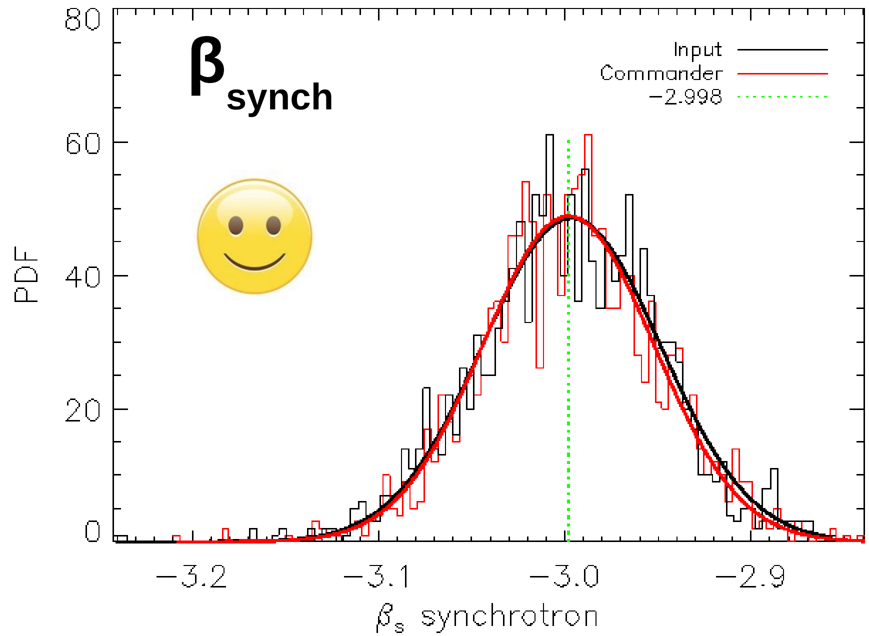

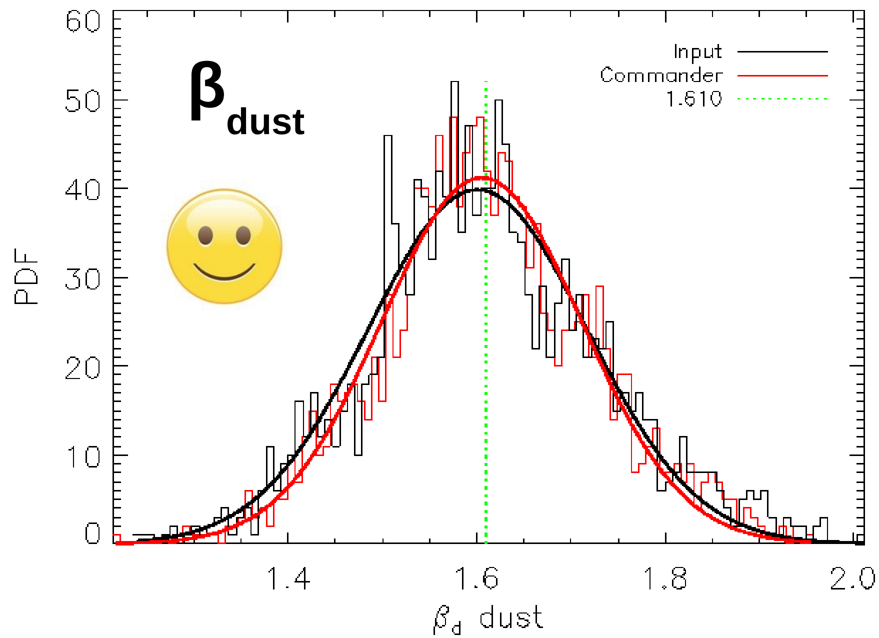

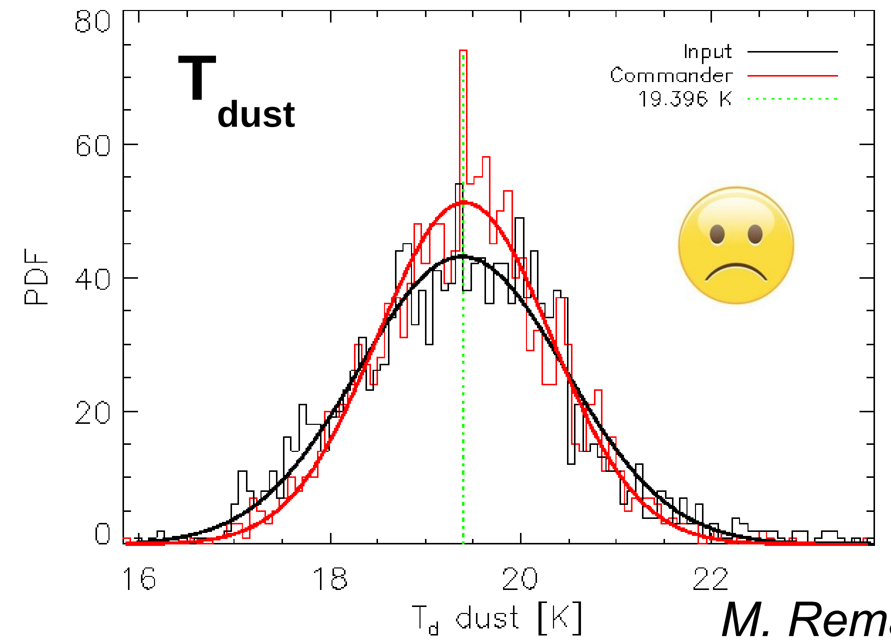

M. Remazeilles

Results for 4D foregrounds (C_s global)
43 – 462 GHz

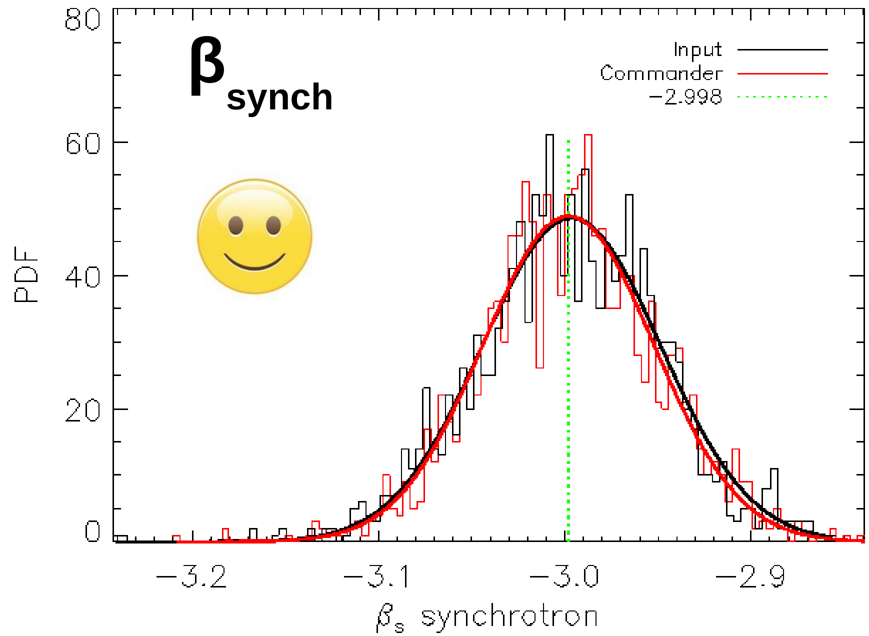

Lack of frequency range / high frequencies

↓

Lack of precision/constraint on T_{dust}

↓

Bias on CMB B-mode by extrapolation toward CMB frequencies

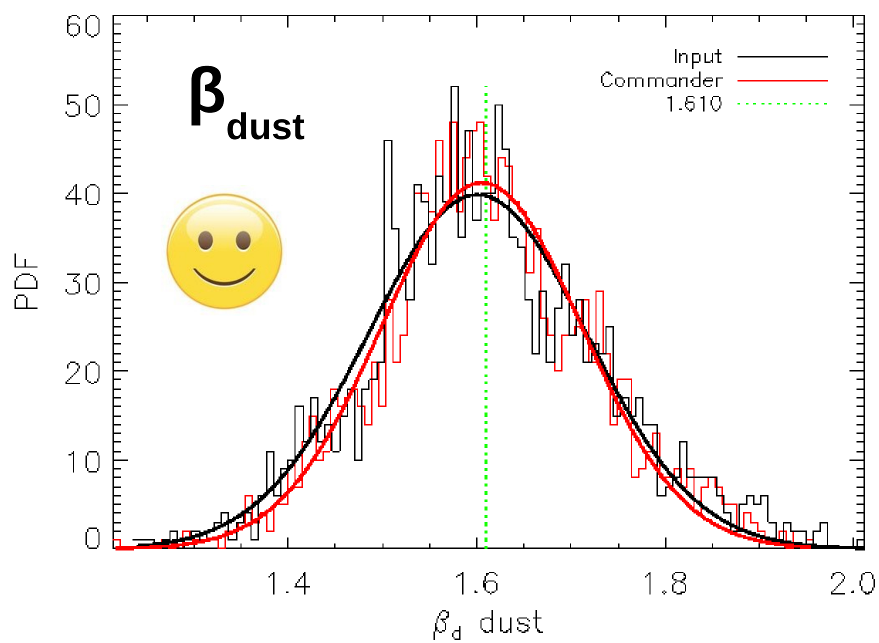

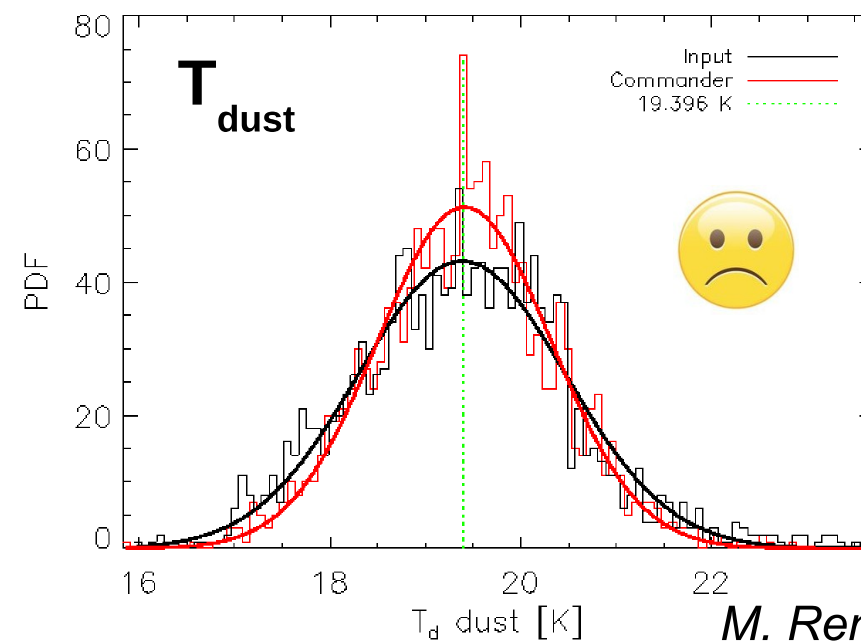

M. Remazeilles

Subtle issues on B-modes

#1. Impact on r of foreground mismodelling

Impact of mismodelling 2 MBB dust components as a single MBB component:

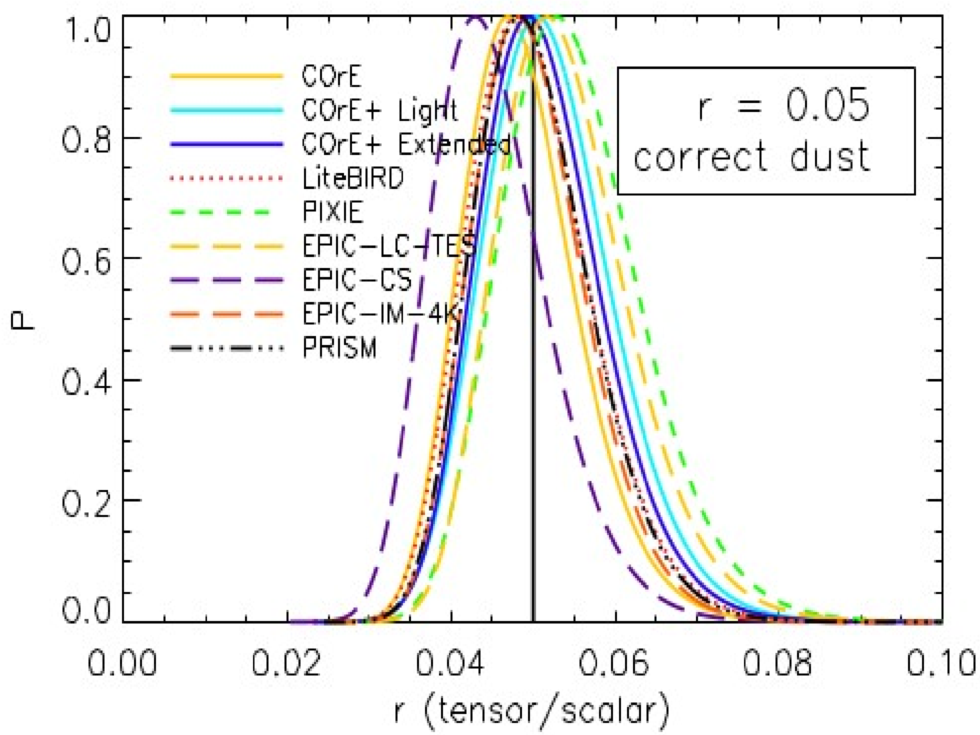

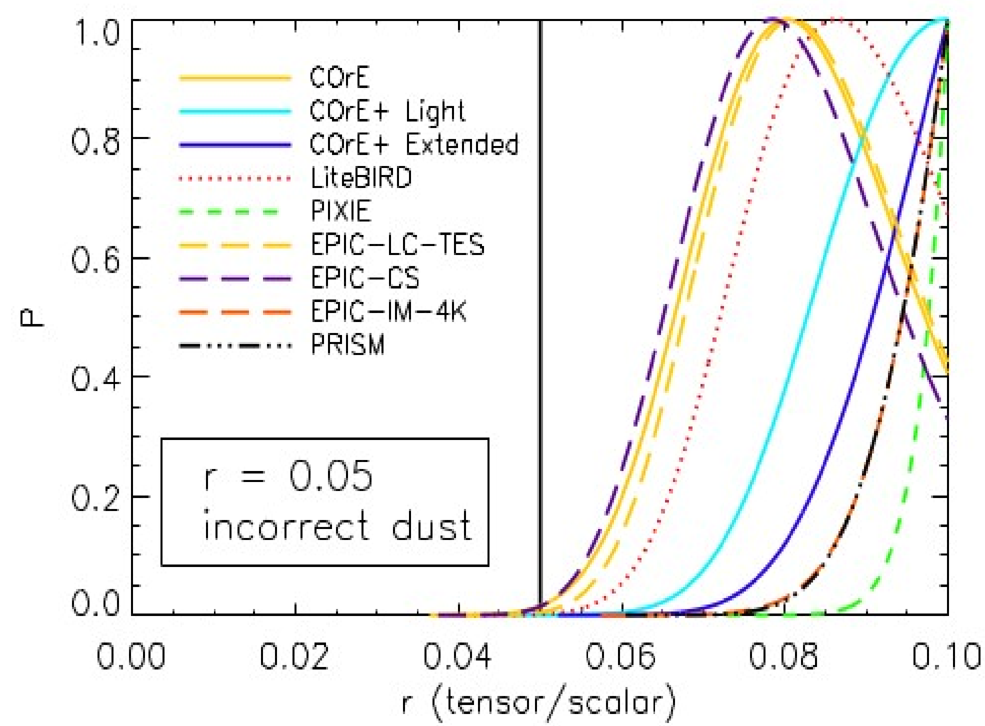

Remazeilles et al, MNRAS 2016

- **How many dust components in the sky? But do we really care?**
- **<u>Most important</u>, what is the actual dust spectrum in the 70 – 140 GHz frequency range?**
- **Any extrapolation is obsolete because of decorrelation effects**

#2. Lack of frequency range / sensitivity to β_s, T_d

Error $\Delta\beta_{synch}$ ~ 0.02 $\Rightarrow$ error Δr ~ 10^{-3} when extrapolated from 23 to 145 GHz !

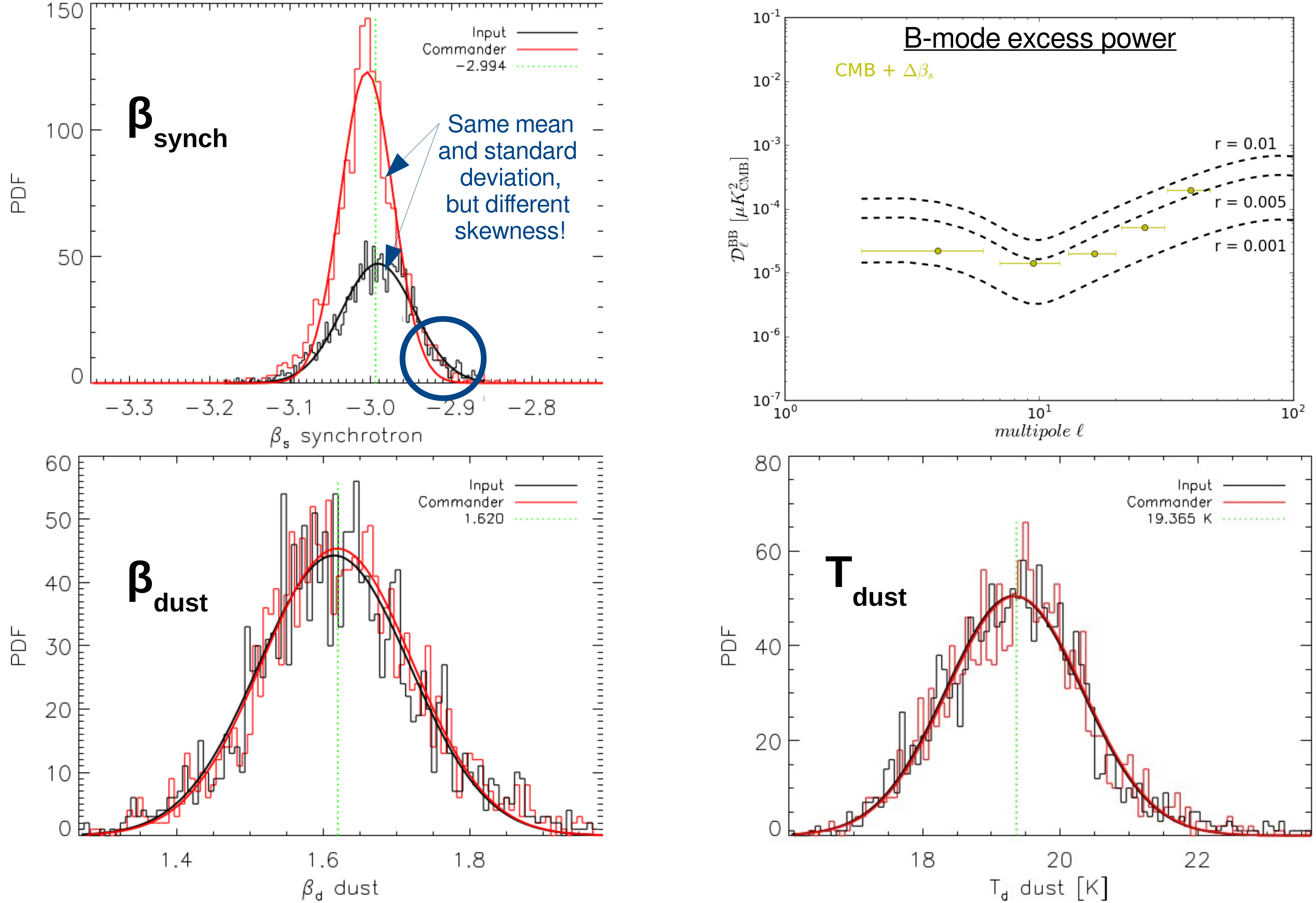

Remazeilles et al, for the CORE collaboration, JCAP 2017
Hervías-Caimapo et al, MNRAS 2017

#3. Averaging effects of spectral indices within pixels / beams

Dust spectral indices in the sky

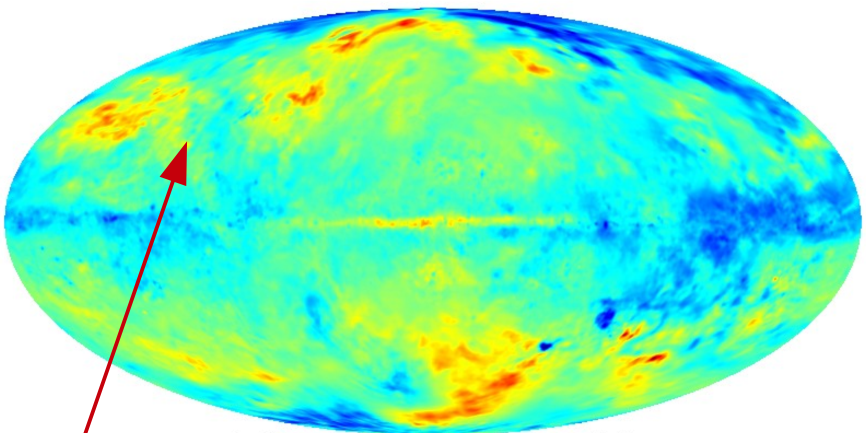

One value β_{dust} per line-of-sight

Map pixelization

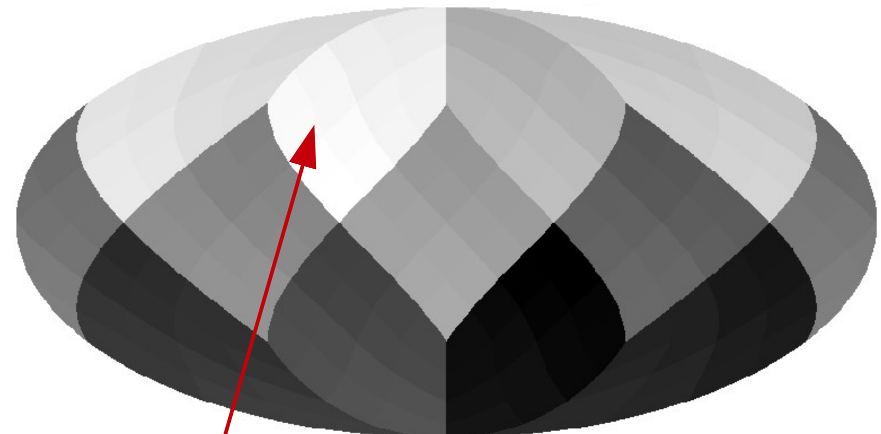

Many values β_{dust} per pixel

(effective SED: $\sum_i \nu^{\beta i} \neq \nu^{\beta}$)

- **Averaging / pixelization creates spurious curvatures on the foreground SED !**
- **The assumed SED might differ from the effective SED in the maps!**

  → source of bias on r = 10^{-3} for parametric / template fitting methods

  → similar to decorrelation effects, but not physical

Chluba, Hill, Abitbol, 2017

Remazeilles et al 2017, for the CORE collaboration

See J. Chluba's talk

#4. Frequency range & spectral degeneracies

- **A bias on r may result from a lack of frequency bands**

(a) Total fit = synchrotron
+ CMB B-mode

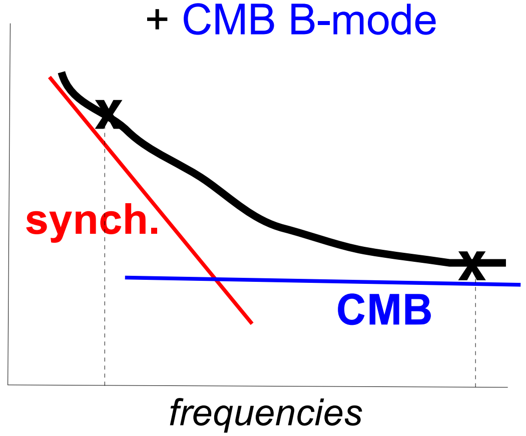

(b) Total fit = curved synchrotron
+ nothing (r = 0) !

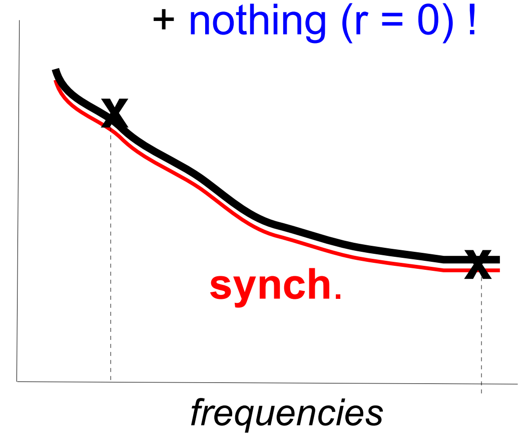

→ Same goodness-of-fit and no chi-square evidence for incorrect modelling!
→ Accurate fit of the total sky emission does not mean correct CMB fit!

- **A bias on r may result from a limited frequency range**

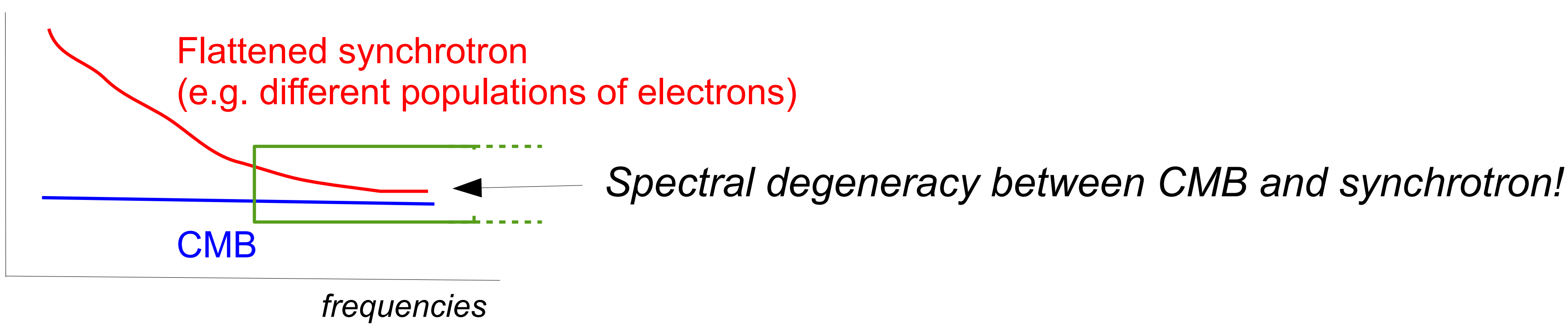

#5. What about magnetic dust (MD)?

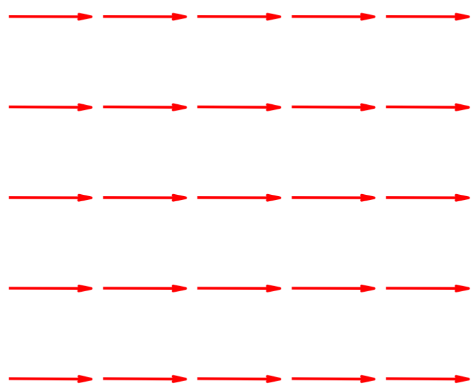

Ferromagnetic lattice with spins aligned.

Thermal fluctuations will move them away, producing magnetic dipole radiation

Draine & Hensley 2013

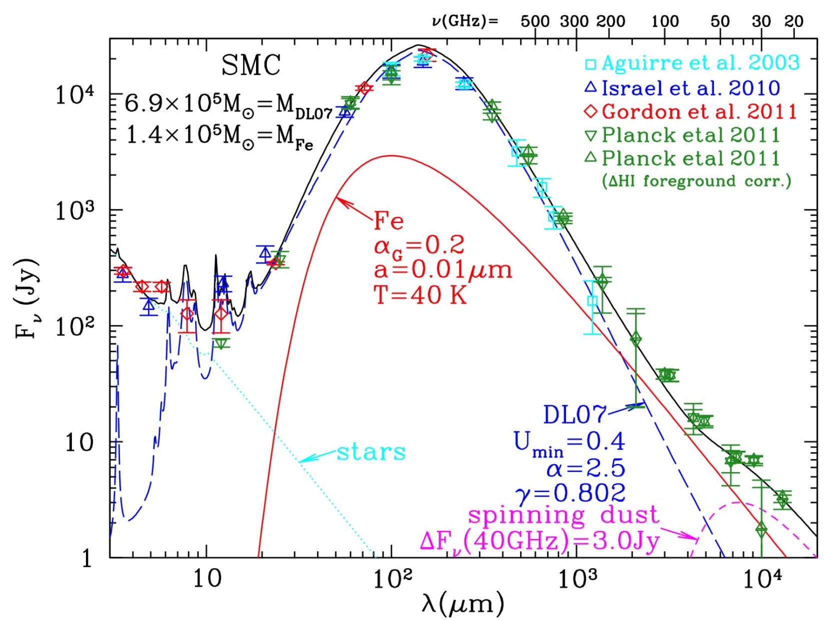

- **Diffuse MD not yet observed!**
- **Theoretically, MD is <u>highly polarized</u> ~35%**
- **MD shows <u>spectral degeneracy with the CMB</u> around 100 GHz!**

  → can be a killer for component separation

See B. Hensley's talk

#6. Extragalactic compact foregrounds

Polarized radio and IR compact sources at ~100 GHz dominate the primordial CMB B-mode at r = 10^{-3} on large angular scales $\ell \gtrsim 50$!

Curto et al 2013

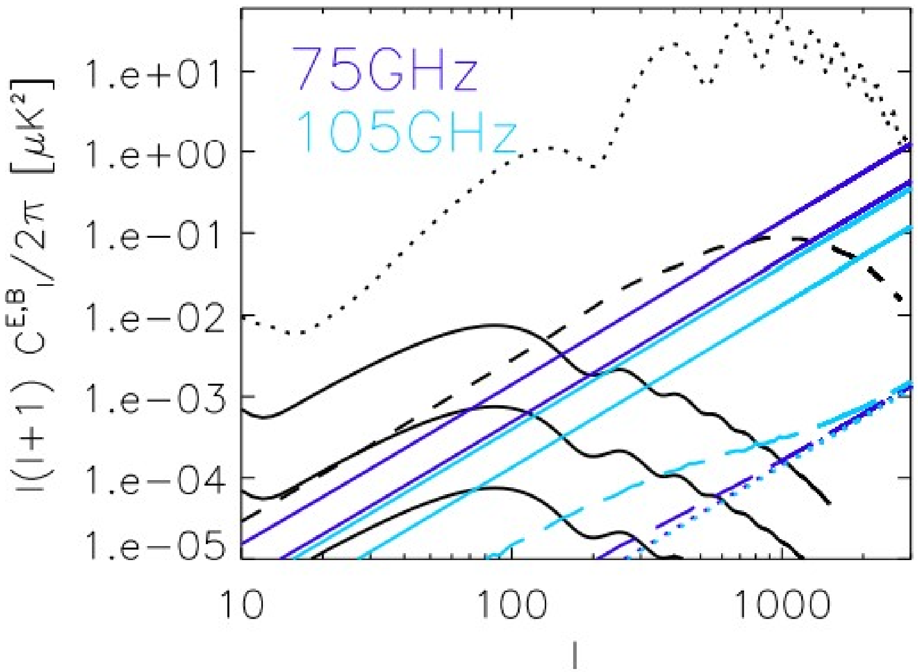

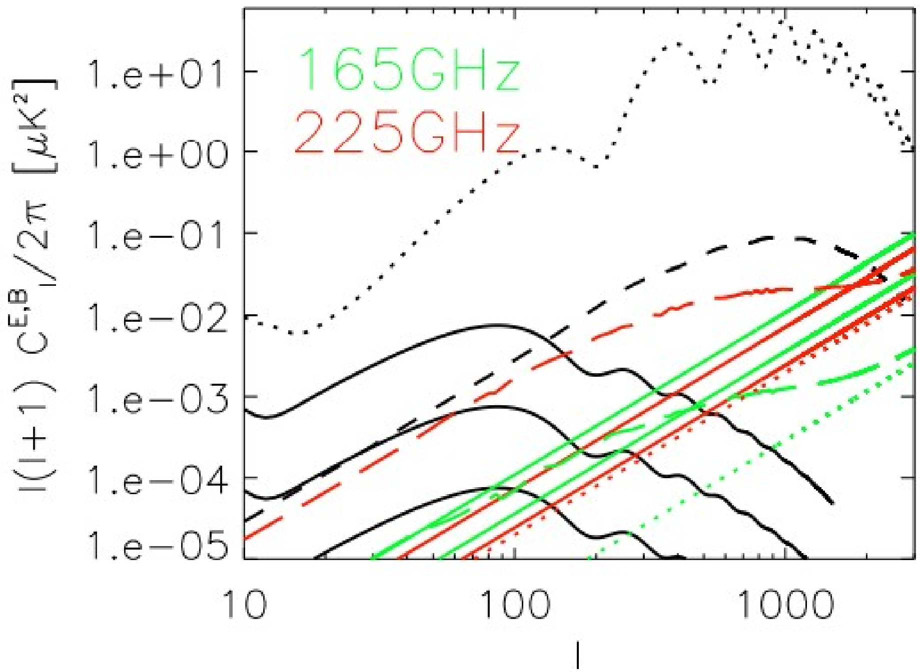

- Detect compact sources in intensity (easier), mask the relevant ones in polarization?
- "Inpainting" of sources in frequency maps prior to component separation?

See G. de Zotti's talk

Sunyaev-Zeldovich effect

NILC : an ILC on wavelets

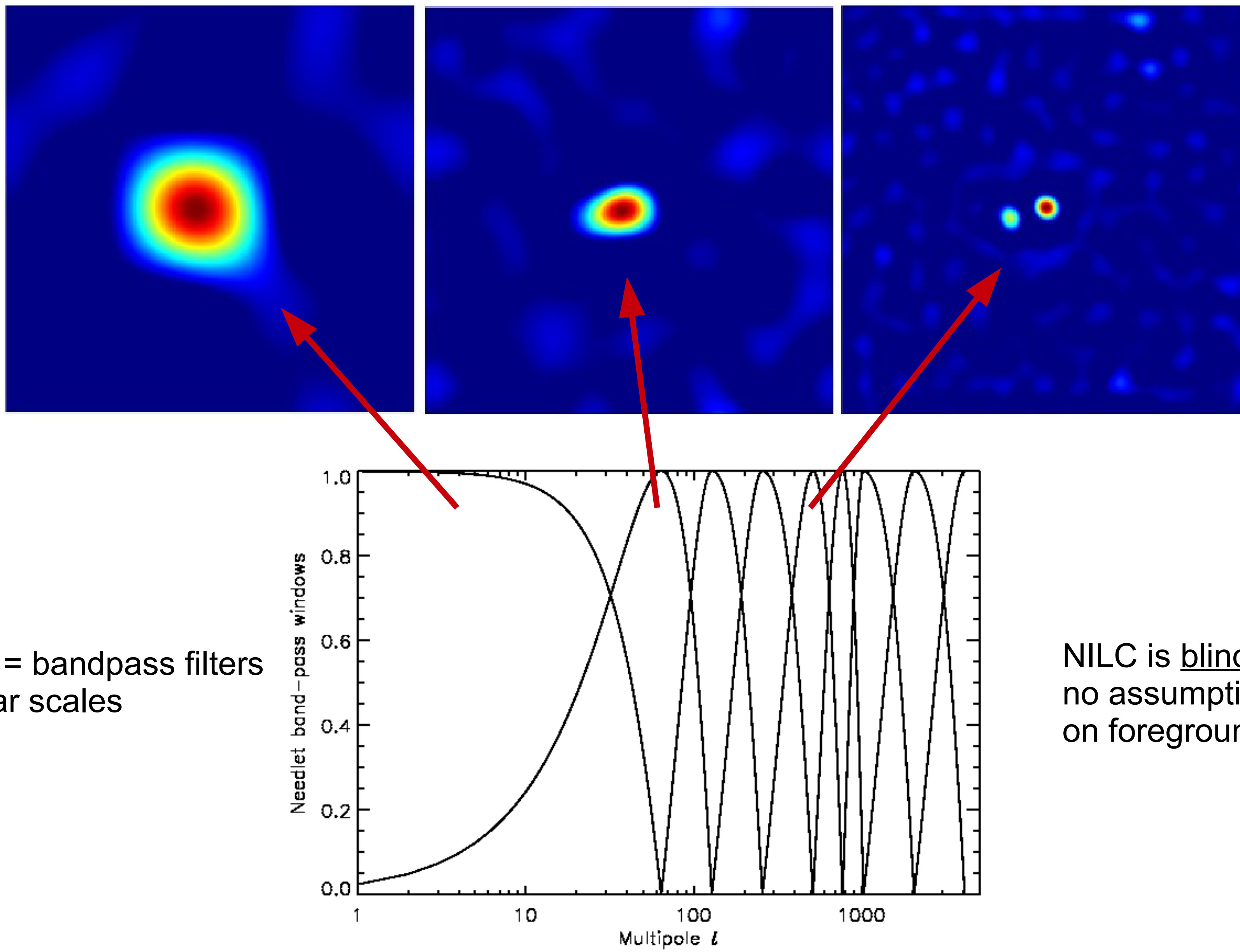

<u>Needlets</u> = bandpass filters on angular scales

NILC is <u>blind</u>: no assumption on foregrounds

Needlets (wavelets) allow to adjust the component separation to the local conditions of contamination both over the sky and over the angular scales

NILC reconstruction of SZ y-map with PICO

Input TSZ map @ 3 arcmin

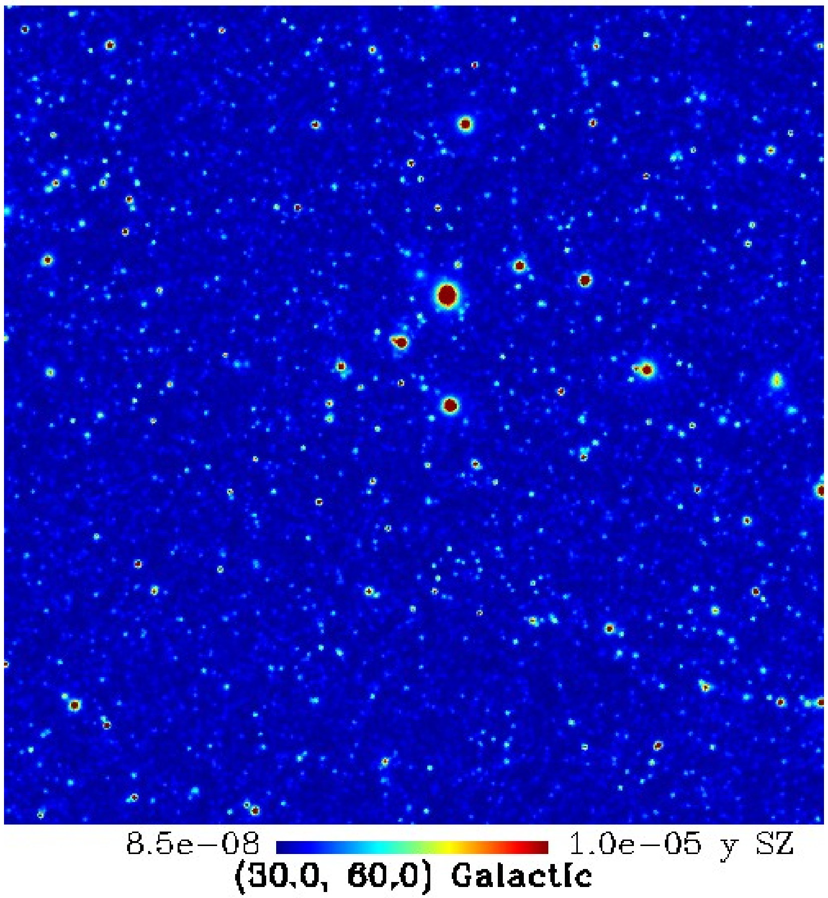

NILC PICO TSZ map @ 3 arcmin

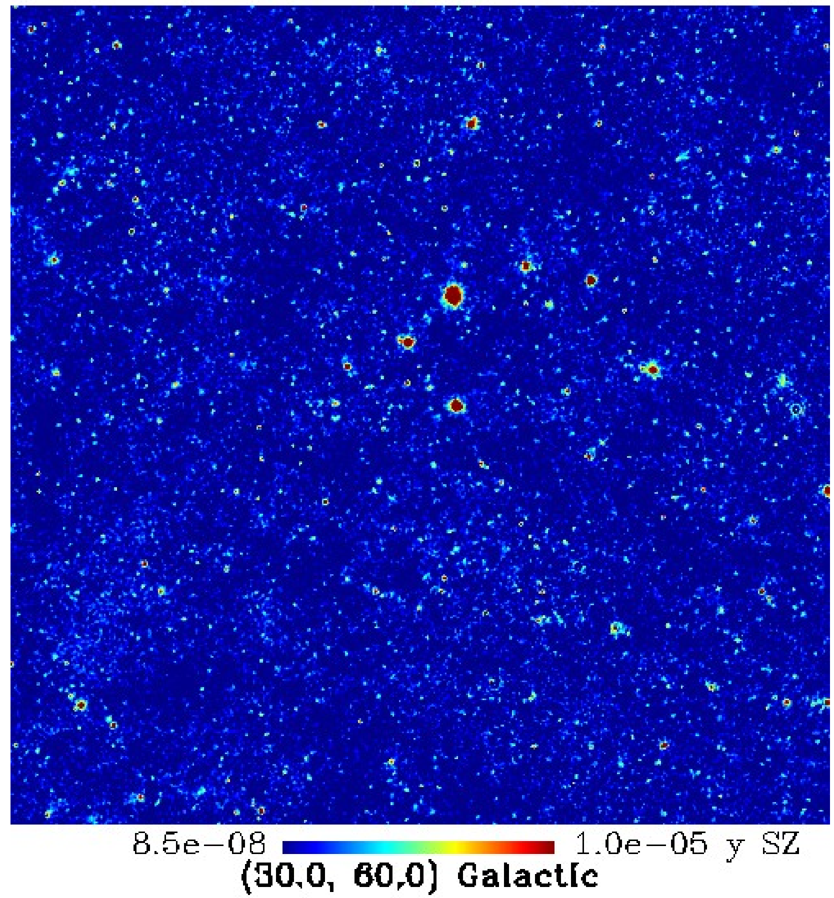

Full-sky PICO NILC y-map available at:

http://www.jb.man.ac.uk/~cdickins/exchange/bpol_sims/Mathieu/CMB-Probe/NILC_Mathieu/PICO_TSZ_NILC_fsky66_res3acm.fits

M. Remazeilles

NILC SZ power spectrum with PICO

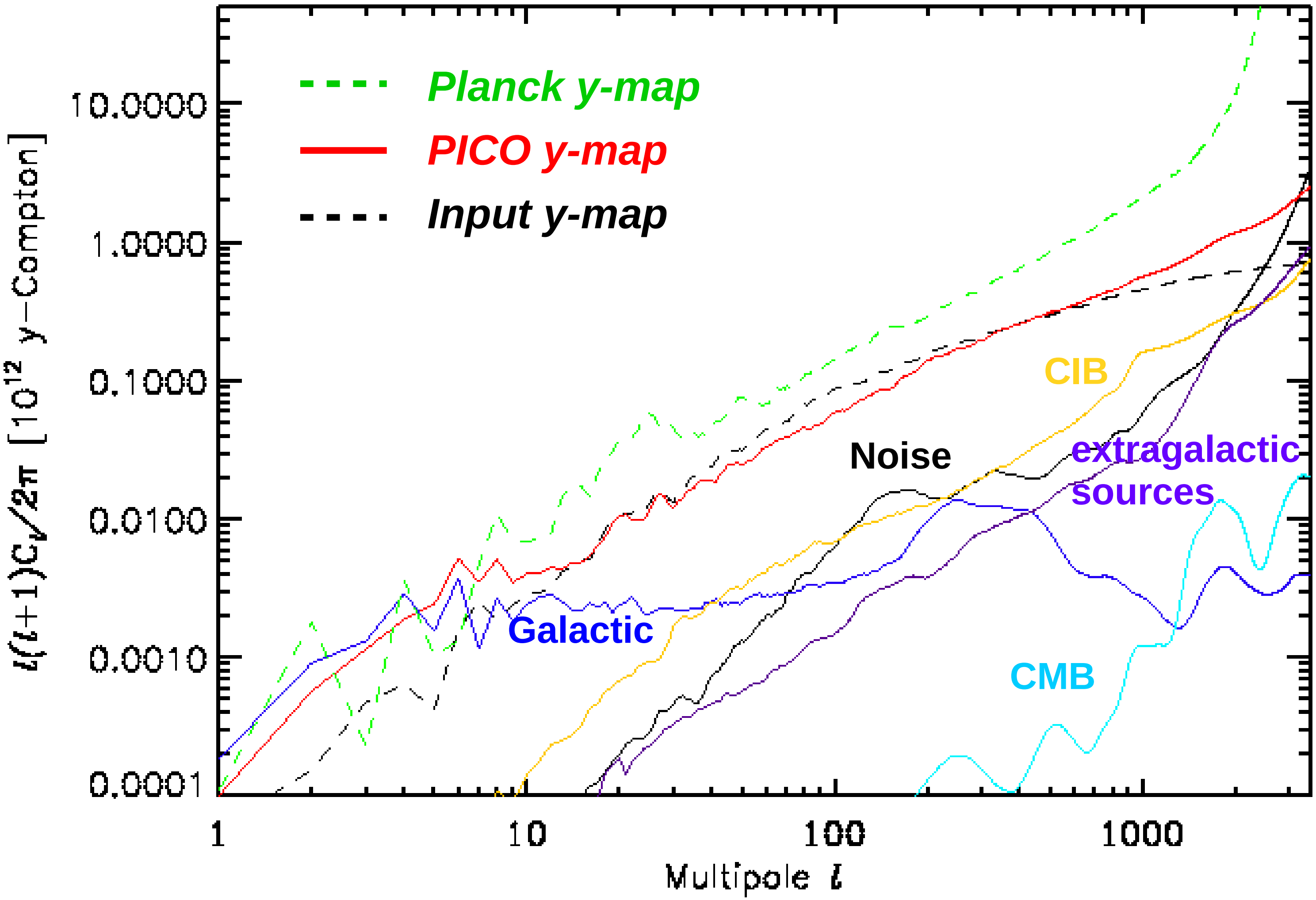

M. Remazeilles

TSZ-free CMB map reconstruction with PICO

Standard NILC

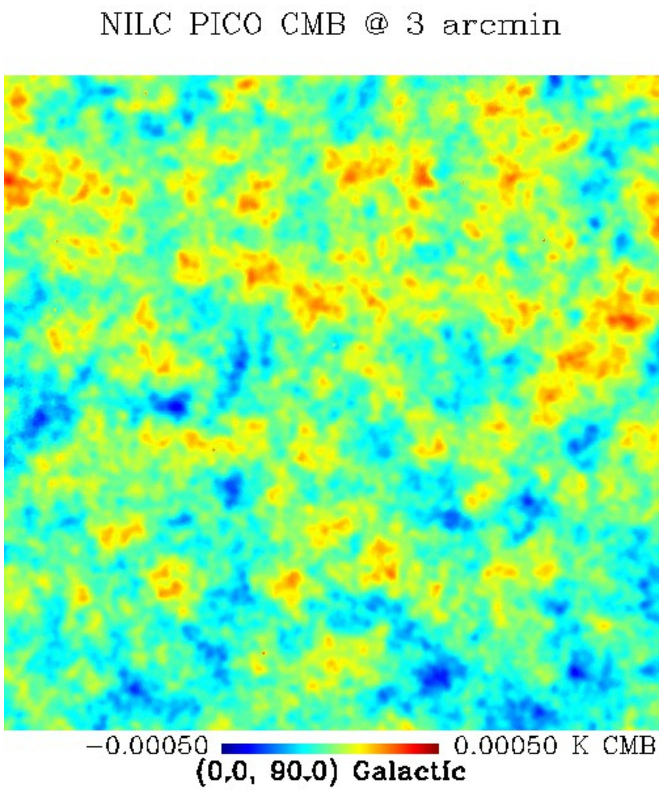

Constrained NILC (SZ-free)

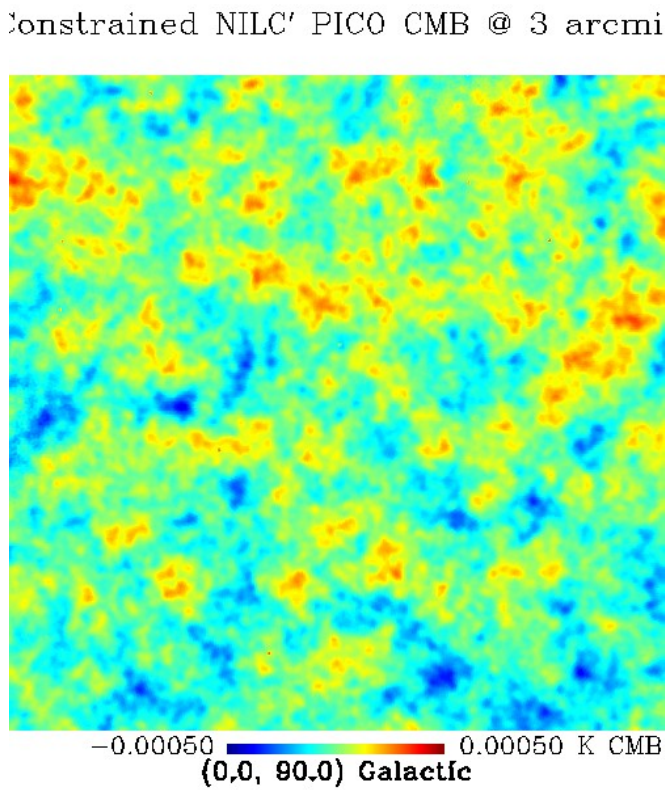

Difference

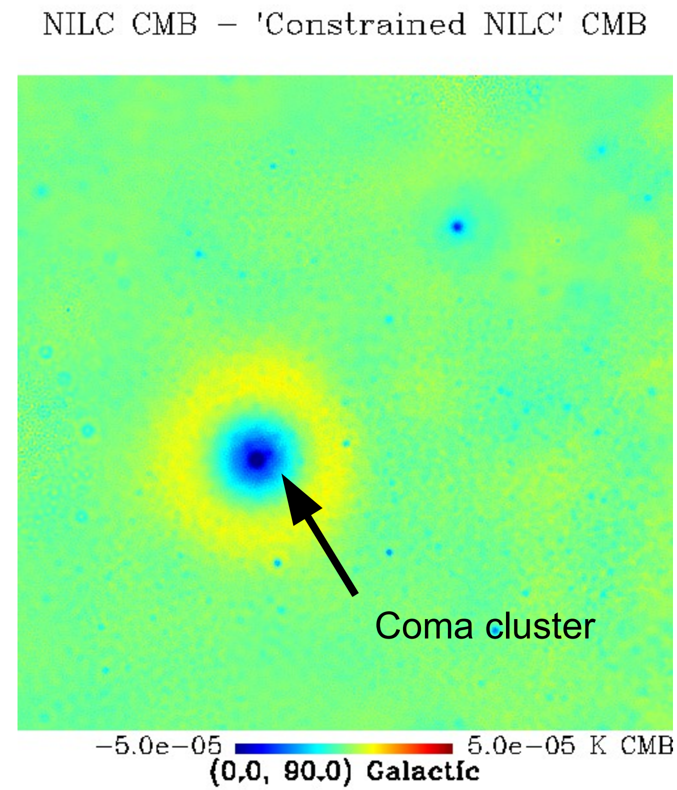

"Constrained NILC" – *Remazeilles, Delabrouille, Cardoso, 2011*

Useful for different scientific objectives:

- Kinetic SZ – *Planck Collaboration Int. XIII, 2014 ; Planck Collaboration Int. LIII, 2017*
- CMB-LSS cross-correlations – *Chen, Remazeilles, Dickinson, in prep.*
- CMB spectral distortions – *Remazeilles & Chluba, in prep.*

M. Remazeilles

PICO TSZ-free CMB map

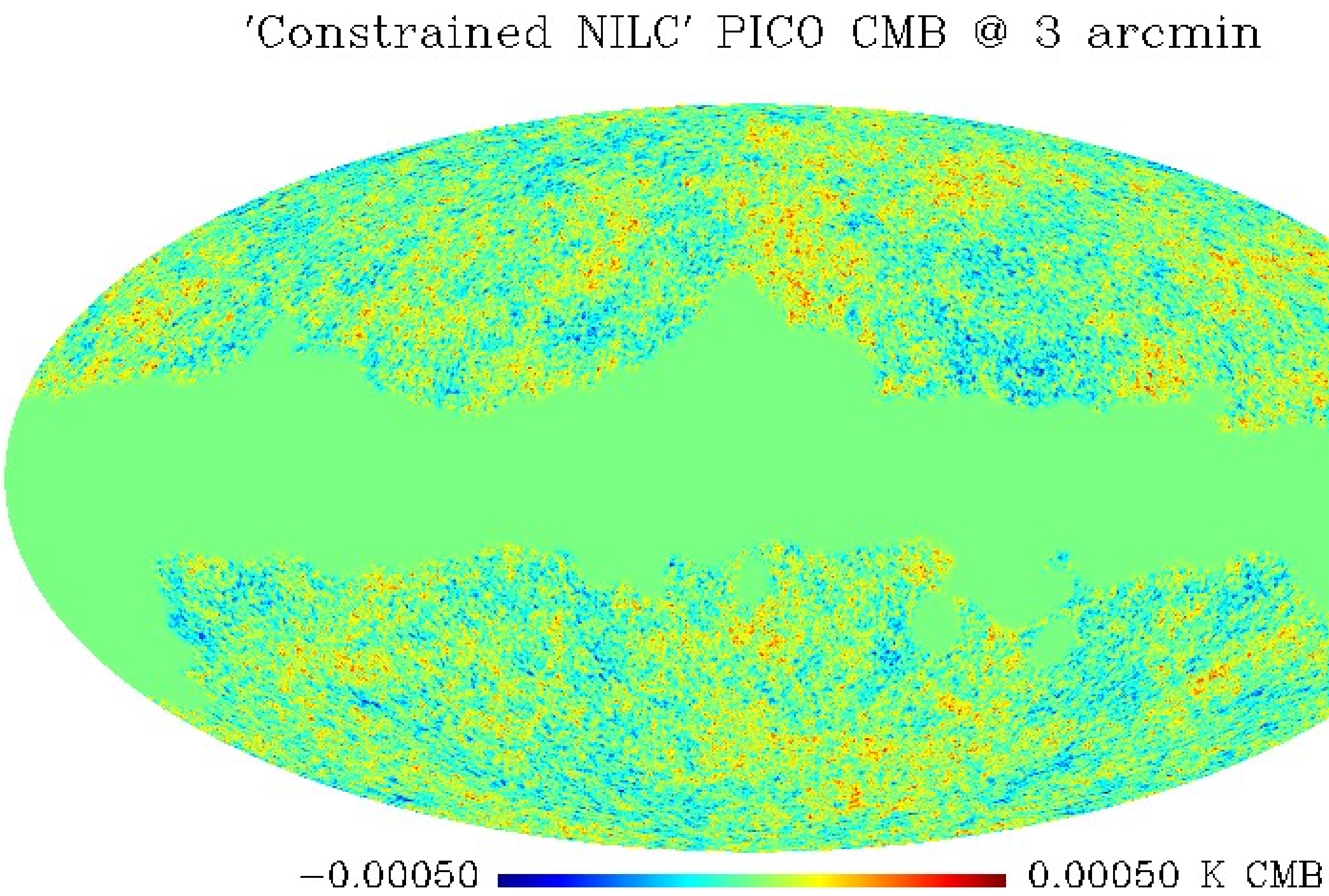

Available at:

http://www.jb.man.ac.uk/~cdickins/exchange/bpol_sims/Mathieu/CMB-Probe/NILC_Mathieu/PICO_CMB_Constrained_NILC_fsky66_res3acm.fits

M. Remazeilles